© 2014. Published by The Company of Biologists Ltd | Journal of Cell Science (2014) 127, 432–444 doi:10.1242/jcs.137786

RESEARCH ARTICLE

Live-cell fluorescence imaging reveals high stoichiometry of Grb2 binding to the EGF receptor sustained during endocytosis

Arola Fortian and Alexander Sorkin*

ABSTRACT

Activation of epidermal growth factor (EGF) receptor (EGFR) leads to its interaction with Grb2, a dual-function adapter mediating both signaling through Ras and receptor endocytosis. We used time-lapse three-dimensional imaging by spinning disk confocal microscopy to analyze trafficking of EGFR and Grb2 in living HeLa cells stimulated with low, physiological concentrations of EGFR ligands. Endogenous Grb2 was replaced in these cells by Grb2 fused to yellow fluorescent protein (YFP). After transient residence in the plasma membrane, Rhodamine-conjugated EGF (EGF–Rh) and Grb2–YFP were rapidly internalized and accumulated in endosomes. Quantitative image analysis revealed that on average two Grb2–YFP molecules were colocalized with one EGF–Rh in cells stimulated with 2 ng/ml EGF–Rh, and the excess of Grb2–YFP over EGF–Rh was even higher when a receptor-saturating concentration of EGF–Rh was used. Therefore, we hypothesize that a single EGFR molecule can be simultaneously associated with functionally distinct Grb2 interaction partners during and after endocytosis. Continuous presence of Grb2–YFP in endosomes was also observed when EGFR was activated by transforming growth factor-α and amphiregulin, suggesting that endosomal EGFRs remain ligand occupied and signaling competent, despite the fact that these growth factors are thought to dissociate from the receptor at acidic pH. The prolonged localization and activity of EGFR–Grb2 complexes in endosomes correlated with the sustained activation of extracellular stimulus-regulated kinase 1/2, suggesting that endosomal EGFRs contribute significantly to this signaling pathway. We propose that endosomal EGFRs function to extend signaling in time and space to compensate for rapid downregulation of surface EGFRs in cells with low receptor expression levels.

KEY WORDS: EGF receptor, Grb2, Endocytosis, Endosome

INTRODUCTION

EGF receptor (EGFR) plays the major role in regulation of proliferation, differentiation, survival and motility of cells during development and in adult organisms (Sibilia et al., 2007). EGFR is overexpressed or mutated in various epithelial cancers, glioma and glioblastoma, and has become an important therapeutic target in several types of carcinoma (Scaltriti and Baselga, 2006). Upon ligand binding to EGFR at the cell surface, receptor dimerization and subsequent activation of its kinase lead to tyrosine phosphorylation of the cytoplasmic domain of the receptor (Lemmon and Schlessinger, 2010). Adaptors and enzymes containing Src homology 2 (SH2)- and phosphotyrosine-binding domains dock to EGFR phosphotyrosines to trigger changes in the signaling network ultimately leading to altered gene expression and transcription-independent effects.

EGFR activated at the cell surface is rapidly internalized into early endosomes. Internalized receptors are either recycled back to the plasma membrane or sorted to late endosomes and lysosomes for degradation (Sorkin and Goh, 2009). Growth factor receptor-bound protein 2 (Grb2) is a unique EGFR-binding SH2 adaptor that plays a key role in both signaling by the receptor and its endocytosis. Src homology 3 (SH3) domains of Grb2 are associated with son of sevenless (SOS), a GTP-exchange factor for Ras (Lowenstein et al., 1992). Recruitment of the GrbB2–SOS complex to EGFR activates Ras and initiates a cascade of phosphorylation reactions resulting in activation of MAPK/extracellular stimulus regulated kinase 1 and 2 (ERK1/2) (Chen et al., 2001). Another SH3-dependent interaction of Grb2 with the E3 ubiquitin ligase Cbl mediates EGFR ubiquitylation, which is involved in endocytosis and required for lysosomal targeting of EGFR (Jiang et al., 2003; Waterman et al., 2002). Degradation of activated EGFR in lysosomes results in downregulation of the receptor and serves as the negative-feedback regulatory mechanism of EGFR signaling (Di Fiore and De Camilli, 2001; Wells et al., 1990).

Endocytosis has also been proposed to be necessary for full and sustained activation of ERK1/2 and several other signaling pathways (reviewed by Miaczynska et al., 2004; Scita and Di Fiore, 2010; Sorkin and von Zastrow, 2009). However, experimental demonstration of the requirement of EGFR endocytosis for ERK1/2 activation and other signaling outcomes remains challenging because specific inhibitors of EGFR endocytosis are not available. To date, literature remains controversial on whether global inhibition of endocytosis decreases, enhances or does not affect EGF-induced signaling processes such as the ERK1/2 activation cascade (Brankatschk et al., 2012; Kranenburg et al., 1999; Sousa et al., 2012; Vieira et al., 1996) (reviewed by Sorkin and von Zastrow, 2002). This controversy is at least in part due to the pleiotropic effects of general inhibitors of clathrin- and dynamin-dependent endocytosis.

The promoting role of endocytosis in signaling is also supported by the concept of a ‘signaling endosome’ (Baass et al., 1995). It is well established in many experimental systems that EGFR remains active in endosomes, and a number of components of the EGFR–Ras–ERK1/2 signaling cascade are associated with endosomes (reviewed by Sorkin and von Zastrow, 2002; Sorkin and von Zastrow, 2009). Most evidence is based on biochemical endosome isolation and immunofluorescence microscopy of perfused liver and cultured cells (Di Guglielmo et al., 1994; Oksvold et al., 2001;

Department of Cell Biology, University of Pittsburgh School of Medicine, Pittsburgh, PA 15261, USA.

*Author for correspondence (sorkin@pitt.edu)

Received 1 July 2013; Accepted 24 October 2013

Journal of Cell Science

Journal of Cell Science (2014) 127, 432–444 doi:10.1242/jcs.137786

Wouters and Bastiaens, 1999) (reviewed by Sorkin and von Zastrow, 2002). Activity of EGFR in endosomes was also observed by live-cell microscopy (Gillham et al., 1999; Sato et al., 2000; Jiang and Sorkin, 2002; Matsuda et al., 2001; Sorkin et al., 2000). All these live-cell studies, however, were performed using cells overexpressing fluorescently tagged components of signaling pathways, such as Grb2, Shc and Ras, and by stimulating cells with high, receptor-saturating EGF concentrations. The distribution of EGFR signaling complexes between plasma membrane and endosomes in cells that do not overexpress EGFR and downstream signaling components, and that are stimulated with low concentrations of EGF (comparable with concentrations of EGF in human plasma and most tissues) is not known. Whether the composition of EGFR complexes with signaling effectors differs at the cell surface and in endosomes is also unclear. An additional level of complexity is that binding of other physiological ligands, such as transforming growth factor-α (TGFα), to EGFR is thought to result in formation of pH-sensitive complexes that dissociate in endosomes, thus leading to inactivation of internalized receptors (Ebner and Derynck, 1991; French et al., 1995). Whether EGFRs occupied by ligands other than EGF and TGFα are active in endosomes is unknown.

Hence, we studied the dynamics of EGFR signaling complexes using Grb2 fused to yellow fluorescent protein (YFP) as a sensor of the EGFR activity. HeLa cells in which endogenous Grb2 was replaced by Grb2–YFP were used as an experimental model. Quantitative microscopic imaging analysis of living cells was performed for the first time in cells with a low density of EGFRs and using low concentrations of EGFR ligands. This analysis revealed that endosomes are the predominant location of multi-Grb2–EGFR complexes in cells stimulated with EGF as well as three other EGFR ligands.

RESULTS

Endosomes are the main intracellular location of EGFR–Grb2 complexes

To examine the localization of Grb2 and EGFR in living cells stimulated with EGF, we used a clonal line of Grb2–YFP-expressing HeLa cells that was generated in our previous studies (Huang and Sorkin, 2005). In these cells, endogenous Grb2 was downregulated by a stably expressed short interfering RNA (shRNA) and shRNA-resistant Grb2–YFP fusion protein was constitutively expressed (supplementary material Fig. S1). The level of Grb2–YFP expression in HeLa-Grb2–YFP cells was approximately twofold higher than that of Grb2 in parental cells; however, this Grb2–YFP concentration is within the range of Grb2 levels in mammalian cells and tissues (Diwan et al., 2000; Nag et al., 2009; Verbeek et al., 1997). HeLa-Grb2–YFP cells have ~25,000 ^{125}I-EGF-binding sites per cell, which is comparable with the EGFR expression levels in fibroblasts, keratinocytes and other non-cancerous mammalian cells of epithelial origin (Carpenter and Cohen, 1979; Imai et al., 1982; Vlodavsky et al., 1978).

Living HeLa-Grb2–YFP cells were imaged using spinning disk confocal microscope at 37°C. In non-stimulated cells Grb2–YFP was diffusely distributed in the cytosol and nucleus. Occasionally, large Grb2–YFP clusters were seen on the bottom of the cells, probably associated with tyrosine phosphorylated proteins in focal adhesions. Injection of EGF conjugated to Rhodamine (EGF–Rh; final concentration 2 ng/ml) into the microscope chamber resulted in rapid binding of EGF–Rh to cells and subsequent recruitment of Grb2–YFP to the plasma membrane, which was particularly evident at cell edges (Fig. 1; supplementary material Movie 1). Grb2–YFP was highly colocalized with small clusters of EGF–Rh at cell edges and in filopodia-like membrane protrusions, and on the flat bottomed surface of cells. After the initial increase in EGF–Rh and Grb2–YFP colocalization in the plasma membrane (first 2–3 minutes), the plasma membrane fluorescence of both proteins rapidly declined. This was accompanied by the accumulation of EGF–Rh and Grb2–YFP in intracellular compartments (endosomes) of a variable size (5–10 minutes).

High-frequency three-dimensional (3D) image acquisition resulted in substantial photobleaching of YFP, thus precluding

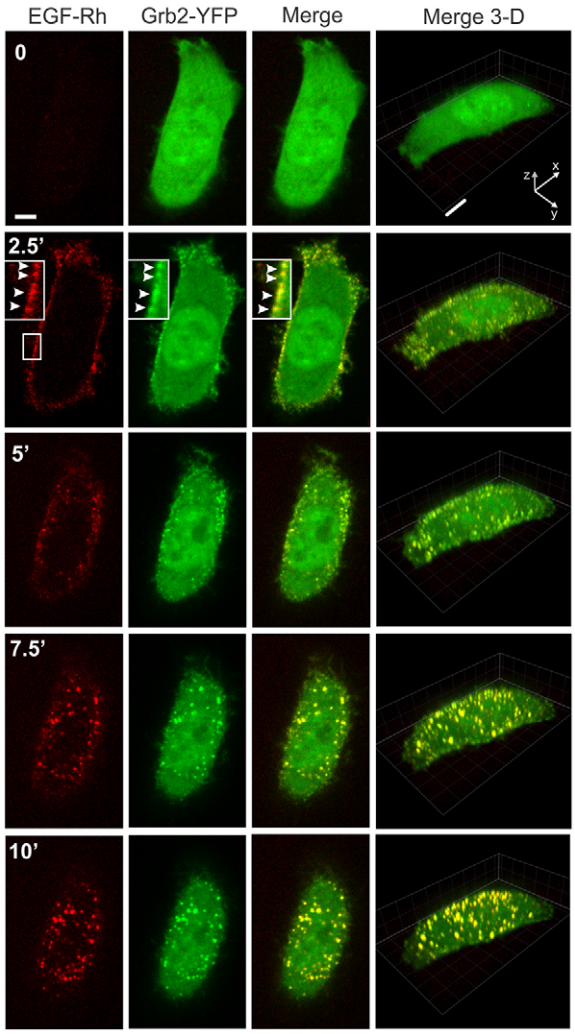

Fig. 1. Time-lapse imaging of Grb2–YFP in cells stimulated with 2 ng/ml EGF–Rh (0–10 minutes). HeLa-Grb2–YFP cells were examined by 3D time-lapse imaging during the first 10 minutes after injection of 2 ng/ml EGF–Rh into the stage chamber at 37°C with 30-second intervals between frames as described in the Materials and Methods. Selected x–y time frames are presented (see corresponding supplementary material Movie 1). Each x–y image of EGF–Rh (red), Grb2–YFP (green) and the merged fluorescence (Merge) is the maximum projection of three neighboring confocal sections. Corresponding merged Rhodamine and YFP images are presented as the complete 3D x–y–z images. Insets are high magnification images of the region indicated by white rectangles. White arrowheads point on the examples of colocalization of EGF–Rh and Grb2–YFP in the plasma membrane. Scale bars: 5 μm.

Journal of Cell Science (2014) 127, 432–444 doi:10.1242/jcs.137786

reliable quantitative image analysis. To monitor and quantify the localization of both EGFR and Grb2–YFP for longer periods of time, and to reduce photobleaching of YFP, 3D images were taken less frequently for 1 hour (Fig. 2; see also supplementary material Movies 2, 3). Strikingly, after ~10 minutes and for the rest of the first hour of incubation with EGF–Rh, most ligand-occupied EGFR and Grb2–YFP were located in endosomes in the majority of cells. Stimulation of cells with higher concentrations of EGF–Rh (4 or 20 ng/ml) produced a qualitatively similar pattern of EGF–Rh and Grb2–YFP traffic, although a proportionally larger pool of total cellular Grb2–YFP was translocated to EGF–Rh containing endosomes (supplementary material Fig. S2). These experiments showed that endosomes are the predominant location of EGFR–Grb2 complexes in HeLa-Grb2–YFP cells stimulated with physiological (2 ng/ml) and supra-physiological concentrations of EGF–Rh (4 and 20 ng/ml).

Using image-segmentation-based analysis of time-lapse sequences (see Materials and Methods), the amounts of colocalized EGF–Rh and Grb2–YFP present in cell-peripheral voxels (plasma membrane) and voxels that are inside of the cell (endosomes) were quantified. This analysis showed that after transient residence at the cell surface, both EGF–Rh and Grb2–YFP accumulated inside the cells whereas less than 10% of fluorescence was associated with cell edges (peripheral voxels; Fig. 3A). Certainly, it is difficult to distinguish surface clusters (clathrin-coated pits and other structures) from peripheral early endosomes using image segmentation, and therefore the data in Fig. 3A are only a rough estimation rather than a precise measurement of the amounts of plasma membrane and endosomal fluorescence. We therefore examined the subcellular distribution of Grb2–YFP in cells stimulated with EGF–Rh using another image analysis method, in which the cell surface was marked by incubating cells with antibodies to the EGFR extracellular domain (mAb528) at 4°C. Following cell fixation, the amounts of Grb2–YFP fluorescence colocalized with mAb528 (plasma membrane) and colocalized with endosomal EGF–Rh were quantified as described in the Materials and Methods. These experiments demonstrated that less than 5% of Grb2–YFP that was colocalized with EGF–Rh was located on the plasma membrane at the 15- to 60-minute time points (Fig. 3B). In summary, two different image analysis methods showed that the majority of EGF-occupied EGFR and receptor-associated Grb2–YFP are located in endosomes after 15 minutes of cell stimulation.

To confirm the dynamics of EGFR endocytosis observed by imaging, the time-course of binding and internalization of ^{125}I-EGF (2, 4 and 20 ng/ml) was analyzed under conditions that duplicated imaging experiments in Figs 1 and 2. As shown in Fig. 3C, ^{125}I-EGF binding to the cell surface was maximal after ~2 minutes of continuous incubation with the ligand at 37°C. The internalization rates during first 5 minutes were similarly high at all ^{125}I-EGF concentrations used, indicating that endocytosis is clathrin mediated. The amount of internalized ^{125}I-EGF increased during the 1 hour incubation when low concentrations of ^{125}I-EGF were used. The internalized ^{125}I-EGF reached a plateau at 30 minutes when 20 ng/ml ^{125}I-EGF was used, suggestive of the full occupancy of receptors. Most important, and similar to what was observed in imaging

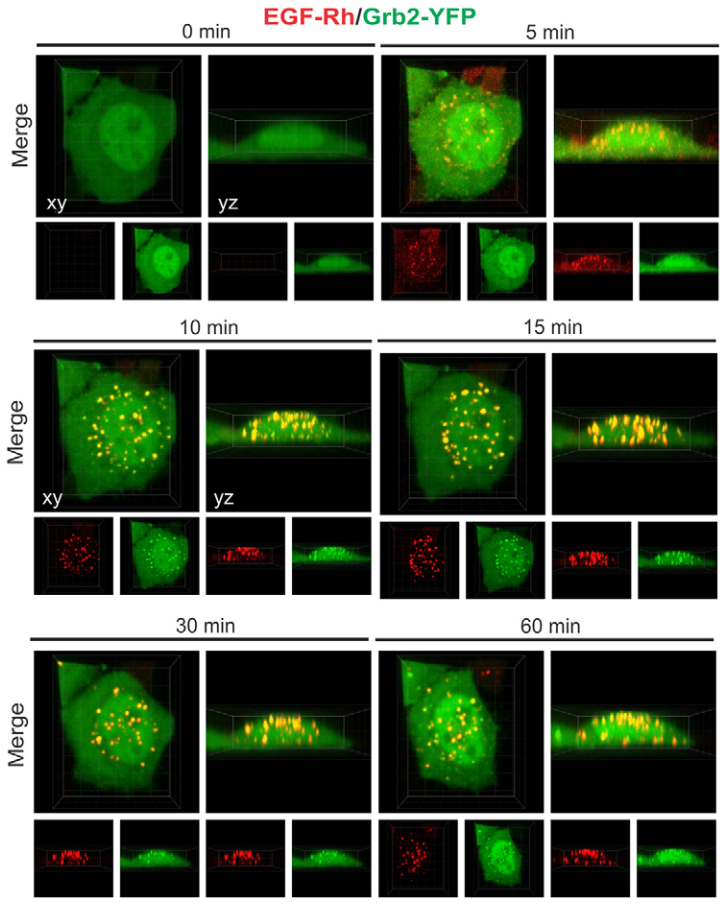

Fig. 2. Time-lapse imaging of Grb2–YFP in cells stimulated with 2 ng/ml EGF–Rh (0–60 minutes). 3D imaging of HeLa-Grb2–YFP cells incubated with 2 ng/ml EGF–Rh at 37°C for the indicated times, as described in the Materials and Methods. Selected x–y and x–z images are presented. See corresponding supplementary material Movies 2 and 3.

Journal of Cell Science (2014) 127, 432–444 doi:10.1242/jcs.137786

experiments, the majority of ^{125}I-EGF–EGFR complexes were located intracellularly after 10 minutes of incubation with the ligand. The residual surface-associated ^{125}I-EGF at later time points is probably the result of incomplete removal of ^{125}I-EGF from cell surface by the acidic wash (Wiley and Cunningham, 1982). Altogether, the data in Figs 1–3 showed that after rapid

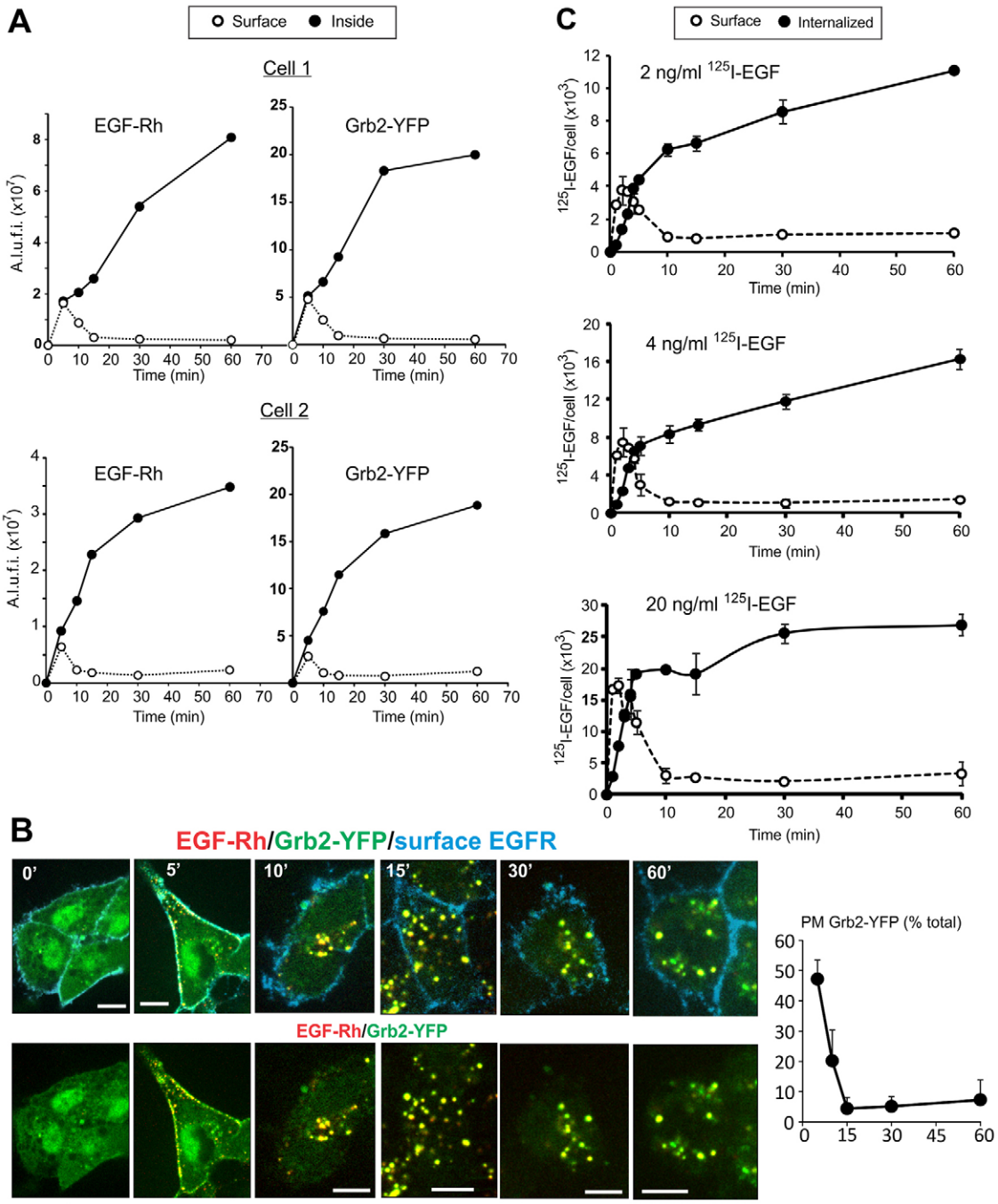

Fig. 3. Quantification of the subcellular distribution of EGFR (EGF–Rh and ^{125}I-EGF) and Grb2–YFP. (A) 3D images of cells incubated with 2 ng/ml EGF–Rh at 37˚C for the indicated times. Two examples of the quantification of the surface (Surface) and endosomal fluorescence (Inside) of EGF–Rh and Grb2–YFP in individual cells are presented. The calculations were performed using mask segmentation-based method described in the Materials and Methods. A.l.u.f.i, arbitrary linear units of fluorescence intensity. (B) The cells were incubated with 2 ng/ml EGF–Rh at 37˚C for the indicated times, and further incubated with mAb528 at 4˚C for 1 hour followed by fixation. Fixed cells were then incubated with the secondary anti-mouse antibody conjugated with Cy5. Merged fluorescence images of Rhodamine (red), YFP (green) and Cy5 (cyan) of individual 3D confocal sections are presented in the top row, and the merged images of Rhodamine and YFP are presented in the bottom row. The percentage of Grb2–YFP associated with the plasma membrane (PM Grb2–YFP) of total Grb2–YFP associated with the plasma membrane and endosomes (total) is shown on the right. The data are mean values (± s.e.m.) from 8–44 cells per data point. (C) HeLa-Grb2–YFP cells were incubated with 2, 4 or 20 ng/ml ^{125}I-EGF for indicated times. The amount of surface and internalized radiolabeled EGF was determined as described in the Materials and Methods and presented as the number of ^{125}I-EGF molecules per cell. Data are compiled from two independent experiments, with two replicates each. Error bars indicate standard deviations of the mean.

Journal of Cell Science (2014) 127, 432–444 doi:10.1242/jcs.137786

transition through the plasma membrane, EGFR and its complex with Grb2 accumulate in endosomes where they reside during most of the first hour of cell stimulation with EGF.

Stoichiometry of the interaction between EGFR and Grb2 in living cells

The predominant localization of EGF–Rh and Grb2 in endosomes prompted us to address whether the composition, and therefore, signaling capacity of EGFR–Grb2 complexes changes during the translocation of EGFR from the plasma membrane to endosomes. Grb2 interactions with EGFR have been previously documented by co-immunoprecipitation in cell lysates, various techniques *in vitro* and fluorescence resonance energy transfer (FRET) microscopy in living cells (Chook et al., 1996; Galperin et al., 2004; Lemmon et al., 1994; Morimatsu et al., 2007; Sorkin et al., 2000). However, these approaches did not provide information on the molar stoichiometry of Grb2–EGFR interactions under conditions of physiological concentrations of these two molecules in living cells. Observations of a nearly absolute overlap of EGF/EGFR and Grb2 localization observed in published and the present experiments (Figs 1, 2; supplementary material Fig. S2), and the demonstration of FRET between EGFR and Grb2 in our previous studies (Galperin et al., 2004; Sorkin et al., 2000) suggest that colocalization of EGFR and Grb2 reflects their direct or indirect interaction. Hence, we assumed that Grb2–YFP colocalization with EGF–Rh reflects direct or indirect association of Grb2–YFP with EGFR, and used the ratio of the fluorescence intensities of EGF–Rh and Grb2–YFP as the measure of the stoichiometry of EGFR–Grb2–YFP complexes (but see caveats of this assumption in the Discussion below).

HeLa-Grb2–YFP cells were incubated with 2, 4 or 20 ng/ml EGF–Rh at 37℃, and 3D images were acquired for only a few time points to minimize photobleaching of YFP. The ratio of YFP and Rhodamine fluorescence was determined in individual compartments (endosomes and plasma membrane clusters) and whole cells. In parallel, experiments were carried out to convert the values of the YFP and Rhodamine fluorescence intensity ratio into the molar ratios of Grb2–YFP and EGF–Rh. To this end, the ratio of the apparent quantum yields of Rhodamine and YFP fluorescence that corresponds to the molar ratio of 1:1 of these fluorophores was determined. Porcine aortic endothelial (PAE) cells that do not express endogenous EGFR were transiently transfected with EGFR–YFP. The cells were incubated with 100 ng/ml EGF–Rh to occupy all receptors (one EGF–Rh per one EGFR–YFP) and imaged under conditions identical to the conditions of experiments with HeLa-Grb2–YFP cells (supplementary material Fig. S3A). The calculations of YFP:Rh ratio in PAE cells yielded a value of ~0.7 (supplementary material Fig. S3B). This value was independent of the amount of EGF–Rh and EGFR–YFP in the cell, thus confirming the linearity of measurements (supplementary material Fig. S3B).

The calculated YFP/Rh coefficient was used to compute the molar stoichiometry of colocalized Grb2–YFP and EGF–Rh during the first hour of cell stimulation with different concentrations of EGF–Rh (Fig. 4A). The amount of Grb2–YFP/cell varied within the population of HeLa-Grb2–YFP cells. The mean Grb2–YFP/cell value ('Total' in Fig. 4B) corresponds to the intracellular concentration of Grb2–YFP that is approximately twofold higher than the steady-state concentration of endogenous Grb2 in parental HeLa cells, as determined by western blot analysis (supplementary material Fig. S1). Therefore, individual cells in which the amount of Grb2–YFP per cell was 30–70% of the mean value of Grb2–YFP/cell (Fig. 4B) were used for calculations of Grb2–YFP:EGF–Rh ratios in Fig. 4A. This range of Grb2–YFP concentrations accounts for a typical variation in protein expression within the population of cultured cells. Surprisingly, calculations of Grb2–YFP:EGF–Rh stoichiometry revealed that more than one Grb2–YFP was associated with one EGFR (considering 1:1 EGF–Rh:EGFR interaction) under all conditions (Fig. 4A). In cells treated with low EGF–Rh concentrations (2 and 4 ng/ml), two or more Grb2–YFP molecules were bound to one EGFR after 5–15 minutes of cell stimulation with EGF–Rh. The highest Grb2–YFP:EGFR stoichiometry was ~3.5:1 when HeLa-Grb2–YFP cells were incubated with 20 ng/ml EGF–Rh. The molar ratios of Grb2–YFP:EGF–Rh were essentially similar in individual endosomes with low and high amounts of EGF–Rh (Fig. 4C), suggesting a relatively homogeneous composition and equal signaling potency of the endosomal complexes, and confirming the linearity of measurements of the intensity and ratio values. siRNA knockdown of Shc did not affect the YFP:Rhodamine ratio in cells incubated with EGF–Rh for 15 minutes (Fig. 4D), suggesting that indirect binding of Grb2 to EGFR through Shc is not significant under experimental conditions used. Because most of the EGFR and Grb2–YFP were located in endosomes after 10–15 minutes of EGF stimulation (Fig. 3), the stoichiometry data suggest that the signaling capacity of EGFR complexes is preserved in endosomes. The stoichiometry of Grb2–YFP binding to EGFR decreased between 15 and 30 minutes of incubation and was then maintained during the subsequent 30 minutes. This decrease is probably due to sequestration of EGF–Rh–EGFR complexes inside multivesicular bodies, a process presumably involving a prior release of adaptors such as Grb2 from the receptor to avoid their lysosomal degradation.

Grb2 is associated with endosomal EGFR, activated by several receptor ligands

The data in Figs 1–4 support the hypothesis that Grb2-mediated signaling is sustained after EGFR internalization in cells treated with EGF. Because other EGFR ligands elicit distinct endocytosis and recycling itineraries of the receptor as a result of the different sensitivity of their receptor binding to the acidic environment of endosomes (Roepstorff et al., 2009), we examined the localization of Grb2–YFP in cells stimulated with three EGFR ligands: TGFα, heparin-binding EGF-like growth factor (HB-EGF) and amphiregulin (AR). To compare the apparent receptor binding affinities of these growth factors in our experimental system, concentration dependence of the displacement of the receptor-bound ^{125}I-EGF by these ligands was analyzed. To this end, the cells were incubated with ^{125}I-EGF (0.5 ng/ml) at 4℃, washed and further incubated with increasing concentrations of unlabeled EGF or other ligands (Fig. 5A). TGFα displayed similar or even higher efficacy in displacing ^{125}I-EGF as compared with unlabeled EGF, suggesting a similar receptor binding affinity of EGF and TGFα at neutral pH. It should be noted that human EGF used in these experiments is known to have a slightly lower receptor binding affinity than mouse EGF used to prepare ^{125}I-EGF and EGF–Rh (Nexø and Hansen, 1985). Higher concentrations of HB-EGF than EGF and TGFα were necessary to have the same effects on ^{125}I-EGF binding, indicative of a slightly lower binding affinity of HB-EGF. Very high concentrations of AR were required to compete out ^{125}I-EGF, suggestive of a very low receptor binding affinity of

Journal of Cell Science (2014) 127, 432–444 doi:10.1242/jcs.137786

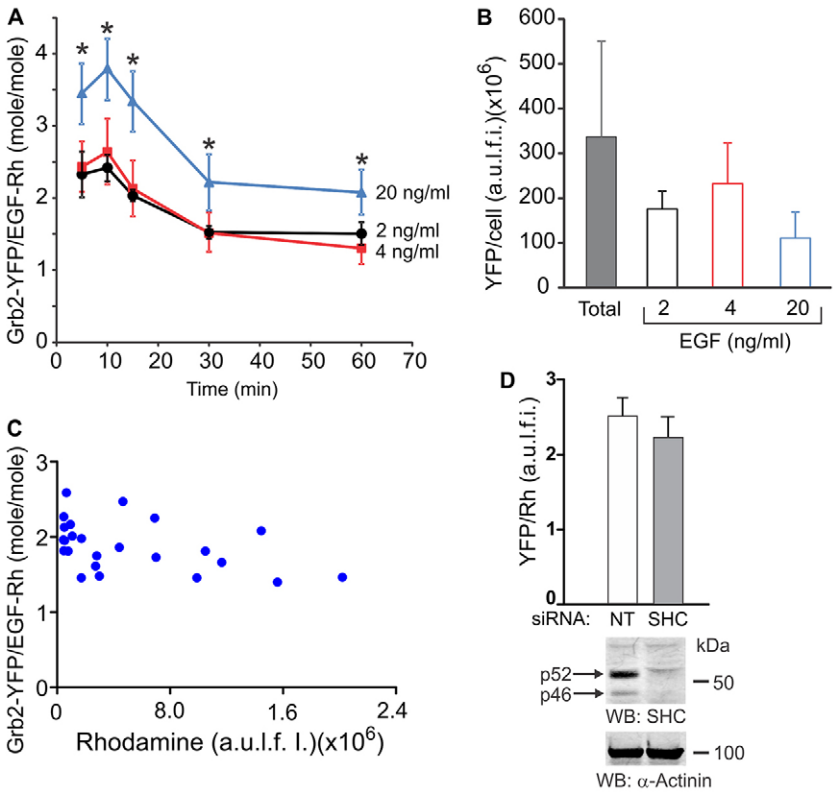

Fig. 4. Molar stoichiometry of colocalized Grb2–YFP and EGF–Rh. (A) Cells were incubated with 2, 4 or 20 ng/ml EGF–Rh for the indicated times. Total cellular YFP and Rhodamine fluorescence intensities were calculated from 3D images acquired as in Fig. 2. Single-cell segmentation-based image analysis was performed to obtain the ratio of Grb2–YFP:EGF–Rh fluorescence intensities in colocalized voxels in individual cells, and values of the Grb2–YFP:EGF–Rh molar ratios in whole cells were calculated as described in Materials and Methods. Error bars represent s.e.m. The data are averaged from five to eight cells at each time point. *$P<0.05$, 20 ng/ml treated cells compared to the corresponding time-points in cells treated with 2 or 4 ng/ml EGF–Rh. (B) The mean amounts of Grb2–YFP per cell in the entire population of cells (total; $n=79$) and in cells treated with 2, 4 and 20 ng/ml EGF–Rh that were used to determine Grb2–YFP:EGF–Rh ratios in A were calculated from 3D images similar to those presented in Fig. 2. Note, Grb2–YFP/EGF–Rh stoichiometry was calculated in A in cells expressing 30–70% lower amounts of Grb2–YFP/cell than the mean Grb2–YFP amount per cell. (C) Representative example of Grb2–YFP:EGF–Rh molar ratios in individual endosomes of a single cell plotted against the amount of the Rhodamine fluorescence per endosome. (D) Cells were transfected with non-targeting (NT) or ShcA (SHC) siRNAs. After 3 days, the cells were incubated with 2 ng/ml EGF–Rh for 15 minutes at 37°C, and the Grb2–YFP:EGF–Rh ratio was measured as in A. The data in the bar graph are mean values (± s.d.) from multiple cells combined from two independent experiments. In parallel, cell lysates were probed by western blotting for Shc and α-actinin (loading control). The blots show efficient knockdown of two major Shc species (p46 and p52) present in HeLa-Grb2–YFP cells.

this commercially available AR preparation. Overall, apparent binding efficiencies of EGFR ligands were consistent with the previously reported data (Ebner and Derynck, 1991; Roepstorff et al., 2009). Hence, imaging of cells was performed using the range of ligand concentrations producing similar extents of ^{125}I-EGF displacement and thus similar levels of the occupancy of surface EGFRs.

Analysis of the subcellular localization of Grb2–YFP complexes revealed that Grb2 was recruited to the plasma membrane and then translocated to endosomes in the presence of low concentrations of TGFα and HB-EGF with the dynamics similar to that of EGF-stimulated cells (Fig. 5). Grb2–YFP accumulated in endosomes to a maximal extent after 15 minutes with practically undetectable plasma membrane localization during the following 45 minutes of incubation with these two ligands. Immunofluorescent staining of EGFR in cells stimulated with various ligands confirmed the large extent of colocalization of Grb2–YFP with EGFR in endosomes (Fig. 6). In cells treated with AR at high concentrations (400–2000 ng/ml; displacing ability comparable to 2–20 ng/ml EGF), Grb2–YFP also accumulated in endosomes, although imaging of cells for more than 30 minutes was precluded because of the apparent toxicity of high concentrations of this AR preparation (Figs 5, 6). Strong colocalization of Grb2–YFP with EEA.1, a marker of early endosomes, was observed in cells treated with all four EGFR ligands for 15 (data not shown) and 30 minutes (supplementary material Fig. S4). A pool of EGFR–Grb2 complexes was also located in endosomes not containing EEA.1 (presumably late endosomes) after 30 minutes of growth factor stimulation. Altogether, the data in Figs 5, 6 and supplementary material Fig. S4 demonstrate that EGFR signaling complexes are present in endosomes regardless of an activating EGFR ligand.

The kinetics of signaling to ERK1/2 and Akt by various EGFR ligands are similar

To compare the kinetics of signaling through two major pathways leading to activation of Akt and ERK1/2 in cells stimulated with different EGFR ligands, HeLa-Grb2–YFP cells were stimulated with EGF, TGFα, HB-EGF or AR in a range of concentrations, resulting in a comparable displacement of ^{125}I-EGF (Fig. 5A). ERK1/2 and Akt phosphorylation (as indicator of their activities)

Journal of Cell Science (2014) 127, 432–444 doi:10.1242/jcs.137786

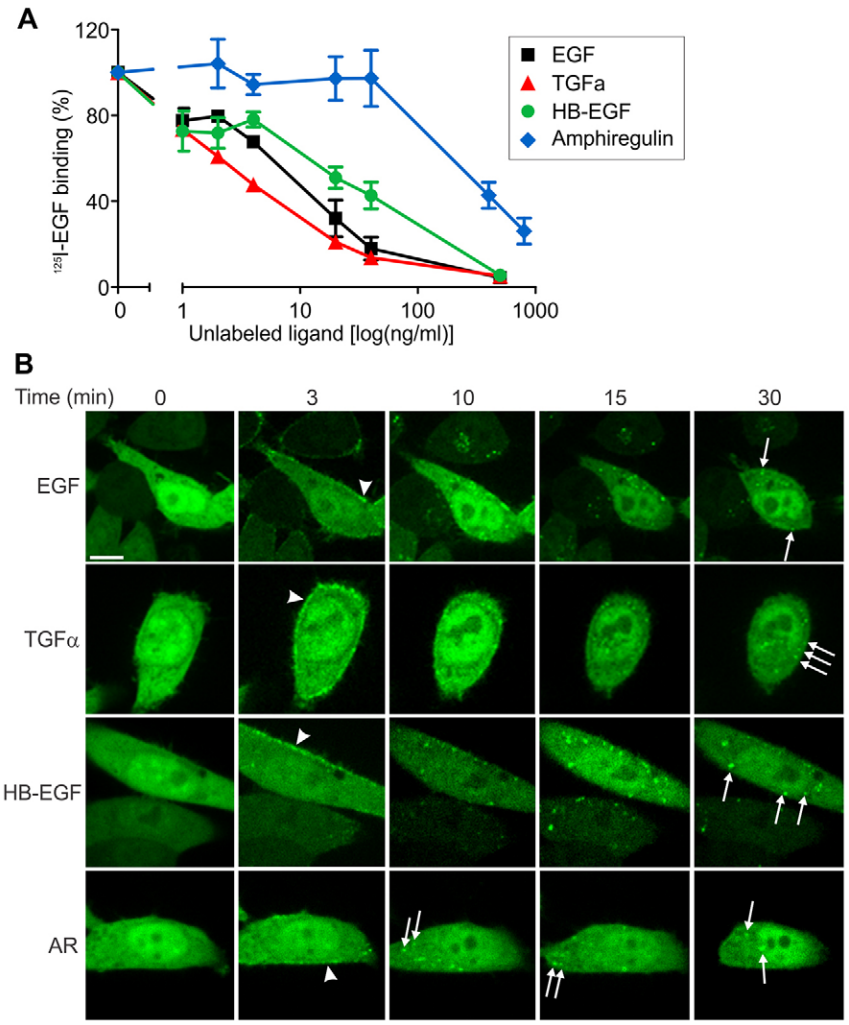

Fig. 5. Different EGFR ligands induce endosomal localization of Grb2–YFP. (A) Dose dependence of ^{125}I-EGF displacement by EGFR ligands. Cells were incubated with ^{125}I-EGF for 1 hour at 4°C, washed with cold DMEM, and further incubated with various EGFR ligands at the indicated concentrations for 1 hour at 4°C. Radioactivity was measured in total cell lysates. (B) Time-lapse images of HeLa-Grb2–YFP cells incubated with EGF (4 ng/ml), TGFα (4 ng/ml), HB-EGF (40 ng/ml) or AR (2 μg/ml) for 0–30 minutes at 37°C. White arrowheads and arrows indicate the examples of localization of Grb2–YFP in the plasma membrane and endosomes, respectively. Each image corresponds to a single confocal section of the 3D image stacks. Scale bar, 10 μm.

was detected by western blotting (Fig. 7A). Under all conditions Akt was activated to a maximal extent during the first 5 minutes followed by ~80% decrease in the activity after 10–15 minutes of growth factor stimulation (Fig. 7B). In contrast, ERK1/2 activity reached maximum at 5–15 minutes after stimulation and slowly decayed during 1 hour of continuous incubation with EGF, TGFα and HB-EGF. Typically, ERK1/2 activity decreased only by about half of the maximal level after incubation for 30 minutes with EGFR ligands, with the exception of faster decay of ERK1/2 activity by 4–20 ng/ml EGF and 40 ng/ml HB-EGF; the latter effects are probably due to an efficient lysosomal targeting of EGFR under these conditions (Roepstorff et al., 2009). Only high concentrations of AR, corresponding to the same binding activity as 2–4 ng/ml EGF and TGFα, were capable of sustained ERK1/2 activation (Fig. 7B). A higher level of sustained activation of ERK1/2 was observed in cells treated with TGFα, possibly because of inefficient lysosomal targeting of EGFR by this ligand as compared to EGF and HB-EGF. Comparison of the data in Figs 5–7 with the results in Fig. 3 and Fig. 4A suggests a correlation of the time-course of Akt activity with the localization of the EGFR–Grb2 complex in the plasma membrane and the time-course of ERK1/2 activity with the endosomal localization of Grb2–EGFR complexes, thus implicating endosomal EGFRs stimulated by various EGFR ligands in signaling to ERK1/2.

To examine the importance of endosomal receptors in supporting the ERK1/2 activity, we took advantage of the observation that at least 90–95% of total cellular EGFR–Grb2 complexes are accumulated in endosomes of HeLa-Grb2–YFP cells after 15 minutes of EGF stimulation (Fig. 3). The cells were stimulated with EGF–Rh for 15 minutes and then treated with a membrane-permeable inhibitor of EGFR kinase activity, PD158780. This treatment led to rapid dephosphorylation of EGFR (Fig. 8A) and release of Grb2–YFP from endosomes containing EGF–Rh, which was evident from an ~50% decrease in the ratio of Grb2–YFP to EGF–Rh in endosomes after 5 minutes of EGFR inhibition (Fig. 8B,C). This data suggests that the bulk of the complexes consisting of EGF–Rh, EGFR and Grb2–YFP are located in the limiting membrane of endosomes, although some Grb2–YFP remains in endosomes because of residual EGFR phosphorylation and/or incorporation of a pool of EGFR–Grb2 complexes into intralumenal vesicles of multivesicular endosomes. Inhibition of EGFR kinase activity also resulted in the dramatic inactivation of ERK1/2 (Fig. 8A). These data suggest that sustained ERK1/2 activity requires upstream signaling by Grb2–EGFR complexes that are located in endosomes.

DISCUSSION

In the present study we used a genetically engineered HeLa cell line expressing fluorescently labeled Grb2 to recapitulate the behavior of EGFR signaling complexes in cells with few EGFRs

Journal of Cell Science (2014) 127, 432–444 doi:10.1242/jcs.137786

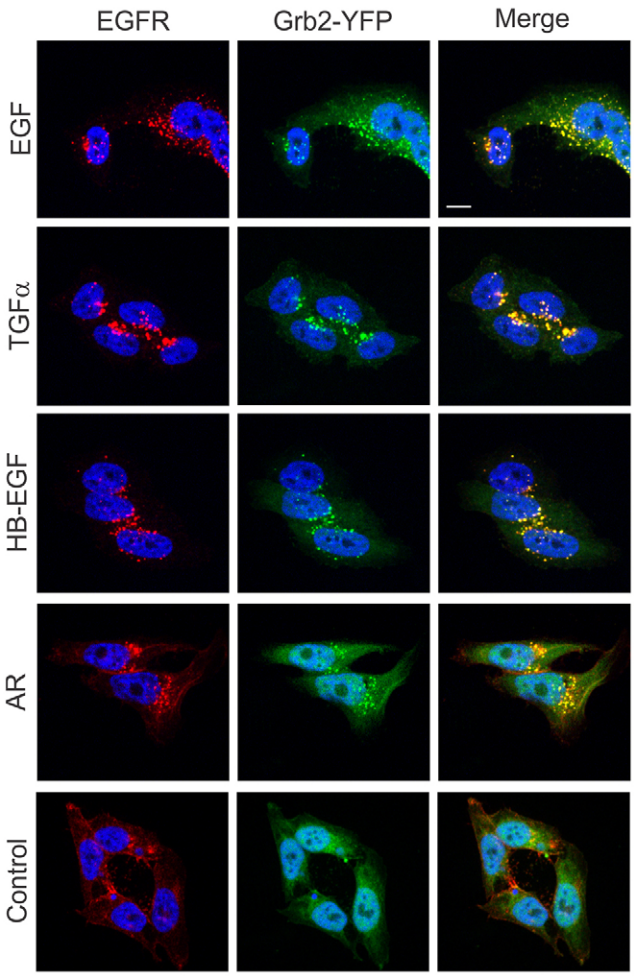

Fig. 6. Colocalization of Grb2–YFP with EGFR in HeLa-Grb2–YFP cells treated with unlabeled EGFR ligands. Cells grown on glass coverslips were left untreated (Control) or treated with EGF (2 ng/ml), TGFα (2 ng/ml), HB-EGF (2 ng/ml) or AR (400 ng/ml) for 30 minutes at 37°C, fixed and stained with mouse monoclonal EGFR (mAb528) followed by secondary antibody conjugated with Cy3. Cell nuclei were stained with DAPI. Scale bar: 10 μm.

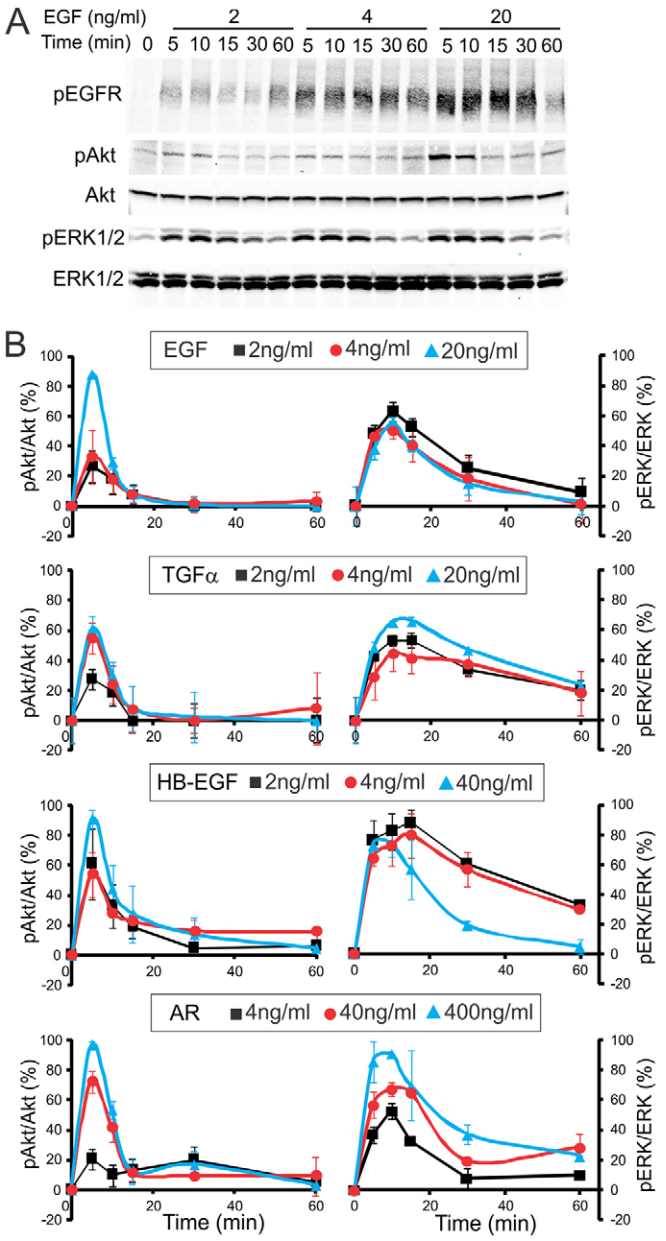

Fig. 7. Kinetics of signaling by EGFR in HeLa-Grb2–YFP cells activated by various receptor ligands. (A) Representative example of EGFR signaling experiments. Cells starved for 16 hours were treated with 2, 4 or 20 ng/ml EGF for the indicated times. Cell lysates were resolved by electrophoresis, and western blotting was performed using antibodies to phosphorylated EGFR (pTyr1068; pEGFR), ERK1/2 (pERK) and Akt (pAkt), as well as pan-ERK1/2 and pan-Akt antibodies. (B) Quantification of western blots from multiple experiments similar to the experiment presented in A. HeLa-Grb2–YFP cells were incubated with different EGFR ligands at the indicated concentrations, as with EGF in A. pERK1/2 and pAkt signals were normalized to the amount of total corresponding proteins. The data are presented as a percentage of the maximal phosphorylation of Akt or ERK1/2 (after subtraction of the signal at time 0) for a given ligand in each experiment. Mean values (± s.e.m.) were calculated from three independent experiments.

and stimulated with low EGF concentrations. Because we noticed in our previous studies that overexpression of Grb2 inhibits EGFR endocytosis (Galperin et al., 2004), it was crucial to express Grb2–YFP at physiological concentrations, so that Grb2–YFP conferred normal EGFR endocytosis and ERK1/2 signaling in Grb2-depleted cells (Huang and Sorkin, 2005). In this experimental model EGFR–Grb2 complexes are predominantly located in endosomes and virtually undetectable in the plasma membrane after 15–60 minutes of EGF stimulation (Figs 1–3). It is probable that the pool of internalized EGF–EGFR complexes capable of recycling is relatively small in HeLa-Grb2–YFP cells. In contrast, recycling is substantial in cells expressing higher levels of EGFR and treated with high concentrations of EGF because of saturation of lysosomal targeting pathways by the large pool of EGFR. Indeed, extensive recycling of EGF–EGFR complexes has been observed in various types of cells with 10^5 or more EGFR/cell (Eden et al., 2012; French et al., 1994; Sorkin et al., 1991). Furthermore, considering that Grb2 is necessary for EGFR ubiquitylation (Huang and Sorkin, 2005; Waterman et al., 2002), the extent of ubiquitylation of EGFR−Grb2–YFP complexes is higher and therefore probability recycling is lower than that of EGFRs not associated with Grb2.

To characterize EGFR−Grb2 complexes, we developed an approach to measure the molar stoichiometry of Grb2 interactions

Journal of Cell Science (2014) 127, 432–444 doi:10.1242/jcs.137786

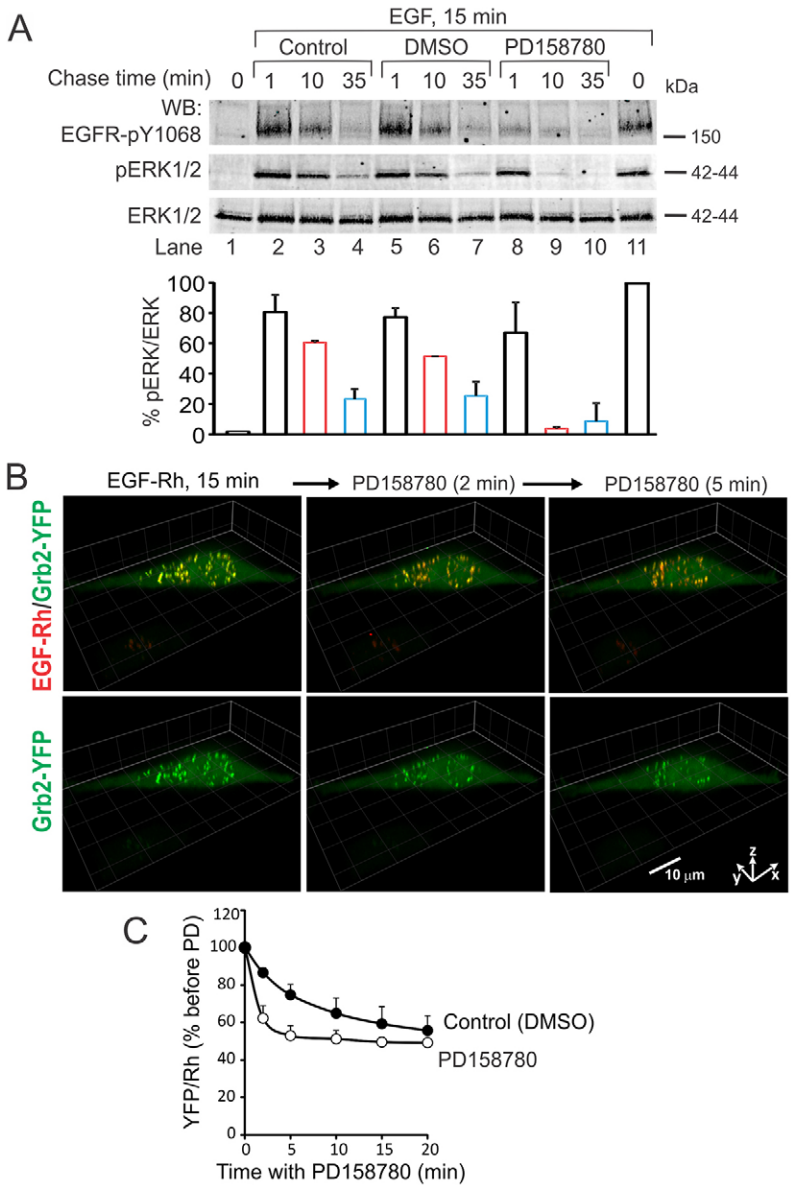

Fig. 8. Effect of the EGFR kinase inhibitor on Grb2–YFP localization in endosomes and ERK1/2 activity. (A) HeLa-Grb2–YFP cells were incubated (lanes 2–11) or not (lane 1) with EGF (40 ng/ml) for 15 minutes at 37˚C. The incubation (Chase) was continued in the same medium (Control, lanes 2–4), or after addition of DMSO (vehicle, lanes 5–7) or PD158780 (50 nM final concentration, lanes 8–10) for additional 1, 10 and 35 minutes. Cell lysates were probed by western blotting with antibodies to pTyr1068 of EGFR (pEGFR), phospho-ERK1/2 and ERK1/2. Bars below blots represent quantification of the ERK1/2 phosphorylation normalized to total ERK1/2 (pERK/ERK), and expressed as a percent of the pERK:ERK ratio in cells treated with EGF for 15 minutes (lane 11). The data are averaged from two independent experiments. (B) HeLa-Grb2–YFP cells were incubated with EGF–Rh (4 ng/ml) for 15 minutes at 37˚C. DMSO (vehicle) or PD158780 were added to EGF–Rh-containing medium, and the cells were further incubated for 0–20 minutes at 37˚C. 3D time-lapse imaging (26 planes, 500 nm intervals) was performed before and after injecting PD158780. Selected time-lapse 3D images are presented. Fluorescence intensity ranges of all images are identical. Scale bar: 10 μm. (C) Quantification of the ratio of YFP and Rhodamine fluorescence intensities in endosomes of cells treated with DMSO or PD158780 as in B was performed as in Fig. 4A. Values are means (± s.e.m.) of YFP:Rhodamine ratios from four to eight cells with similar expression levels of Grb2–YFP.

with EGFR in living cells, and observed surprisingly high Grb2:EGFR stoichiometry, such as ~2:1 and 3.5:1 in cells treated with 2–4 ng/ml and 20 ng/ml EGF, respectively (Fig. 4A). The molar ratios of Grb2 per activated EGFR may even be underestimated because not all EGF–Rh occupied receptors are phosphorylated at the major Grb2-binding sites, Tyr1068 and Tyr1086. It is unclear whether these two binding sites can simultaneously recruit two Grb2 molecules to the same EGFR molecule. Alternatively, Grb2 can bind to EGFR indirectly through Shc or other adaptors (Batzer et al., 1994; Okabayashi et al., 1994; Okutani et al., 1994), although our experiments suggested that the contribution of Grb2 binding to EGFR through Shc is minimal (Fig. 4). High concentrations of EGF may increase the fraction of receptors phosphorylated at tyrosines 1068 and 1086 or other tyrosines that can serve as cryptic Grb2-binding sites (Schulze et al., 2005), thus resulting in increased Grb2:EGFR stoichiometry. Indeed, a Y1068/1086F EGFR mutant transiently overexpressed in PAE cells still binds overexpressed Grb2–YFP (data not shown). The existence of multiple Grb2-binding sites on EGFR is a likely explanation of the very high Grb2:EGFR molar ratios (up to 8) in HeLa-Grb2–YFP cells expressing high amounts of Grb2–YFP (data not shown). Another possible explanation of the high apparent stoichiometry of Grb2 relative to EGF is the proposed existence of EGFR dimers bound to one EGF (Adak et al., 2011; Alvarado et al., 2010). However, because the highest stoichiometry (3.5:1) was observed using a saturating EGF–Rh concentration (20 ng/ml; Fig. 4A), when a pool of complexes consisting of 1 EGF:2 EGFR is predicted to be negligible, the excess of bound Grb2 relative to EGFR is not due to these intermediate dimer species. Furthermore, analysis of EGFR dimerization using high-resolution imaging revealed that 1 EGF:2 EGFR dimers are short-lived and represent a small fraction of the total pool of dimers, and predicted that these complexes are less efficient at initiating signal transduction than 2:2 EGF–EGFR complexes (Low-Nam et al., 2011). Finally, EGFR–ErbB2 heterodimers would have one EGF–Rh bound to a heterodimer, with each monomer having Grb2-binding sites, and this may account for the high number of Grb2–YFP per ligand.

Journal of Cell Science (2014) 127, 432–444 doi:10.1242/jcs.137786

However, the pool of these heterodimers is very small compared with EGFR homodimers in HeLa cells (Johannessen et al., 2001). Additionally, ErbB2–EGFR heterodimers are proposed to be internalization impaired (reviewed by Sorkin and Goh, 2009), thus resulting in preferential endosomal accumulation of EGFR homodimers. Therefore, EGFR heterodimerization may not significantly influence our quantifications of Grb2:EGFR stoichiometry in endosomes. Regardless of the mechanisms responsible for the assembly of multimolecular Grb2–EGFR complexes, it can be hypothesized that two or more Grb2 molecules associated with different SH3 binding partners, such as Cbl, SOS and dynamin, may directly or indirectly bind to a single EGFR or an EGFR dimer, thus conferring ubiquitin-dependent sorting and Ras-mediated signal transduction by the same minimal receptor-signaling unit.

Observation of the sustained high stoichiometry of Grb2 binding to EGFR after internalization suggests that EGF is not significantly released from the receptor and that receptor dephosphorylation is not increased in early endosomes. While the same stability of internalized ligand-receptor complexes and the activity of endosomal HB-EGF–EGFR complexes could be predicted based on the low sensitivity of this complex to acidic pH, accumulation of EGFR–Grb2 complexes in endosomes of cells stimulated with TGFα and AR was surprising (Figs 5, 6). The dissociation rates of TGFα and AR are shown to be high at pH less than 7, and these ligands are expected to dissociate in the acidic environment of endosomes (Roepstorff et al., 2009). Thus the presence of receptor complexes in endosomes is probably because of the shift of binding equilibrium towards association. Calculations based on the number of EGF–Rh-containing endosomes in a HeLa-Grb2 cell detectable under our imaging conditions (~25–60), their average size (0.2–1.0 µm in diameter) and the amount of EGF–Rh per endosome (from 30 to 1000; on average 100–200 per endosome) using 3D images of cells treated with 2 ng/ml EGF–Rh for 15 minutes yields an average concentration of EGF–Rh in endosomes of ~200–400 nM. This range of concentrations is several orders of magnitude higher than the extracellular EGF–Rh concentration (0.34 nM; 2 ng/ml). Given similar rates of receptor endocytosis induced by TGFα and EGF, and a similar number of EGFR–Grb2–YFP-containing endosomes per cell (Figs 5, 6), it is likely that the TGFα concentration in endosomes is as high as that of EGF, which would result in a substantial amount of TGFα remaining associated with receptors in endosomes. The same considerations may be applied to explain the presence of AR–EGFR complexes in endosomes, although much greater concentrations of extracellular AR are required to achieve a significant occupancy of surface EGFRs.

Whether endosomal signaling complexes are involved and/or essential for EGFR signaling has been under extensive debate during the last decade. Although the original study using a dominant-negative dynamin mutant demonstrated that endocytosis is necessary for the full ERK1/2 activation (Vieira et al., 1996), there have been many examples of later studies that used general inhibitors of endocytosis and reached contrasting conclusions regarding the role of the endosomal signaling. For example, a recent study of fibroblasts with a genetic knockout of dynamin 1 and 2 showed that endocytosis is not necessary for the EGFR–ERK1/2 signaling cascade (Sousa et al., 2012). In our previous work internalization-impaired EGFR mutants exhibited normal or enhanced ability to activate ERK (Goh et al., 2010). Given the caveats of using endocytosis inhibitors that are not specific for EGFR, and EGFR mutants that are not completely absent in endosomes, the present work focuses simply on a correlative comparison of the localization and activity of EGFR signaling complexes with the time course of Akt and ERK activation (Figs 7, 8). In agreement with many reports, Akt activity decays very rapidly after stimulation of cells with growth factors, and the time courses of plasma membrane localization of EGFR–Grb2 complexes overlap very well with time courses of Akt phosphorylation (compare Fig. 3 and Fig. 7). This is consistent with the notion that an upstream p85/110 phosphoinositide 3-kinase functions in the plasma membrane but not in endosomes (Haugh and Meyer, 2002). ERK1/2 remains phosphorylated and this phosphorylation depends on the EGFR activity under conditions when most, if not all, EGFR–Grb2 complexes are in endosomes and very few of these complexes are on the cell surface (Fig. 3; Fig. 4A,B; Figs 7, 8). Therefore, it is likely that endosomal EGFRs play an important role in signaling to ERK1/2 in HeLa-Grb2–YFP cells and other cells with low EGFR expression levels. However, it is also likely that endosomal signaling is not quantitatively or qualitatively different from signaling at the cell surface, and that it serves to prolong signaling rather than it is absolutely necessary for ERK activity. In summary, endosomal signaling by EGFR may function in a manner similar to memory through the extension of signal transduction process in time and space under conditions of low extracellular concentrations of growth factors, depletion of these factors by endocytosis and rapid ligand-induced downregulation of receptors from the cell surface. This function of endosomes might be crucial in cells with low levels of EGFR expression but less vital in cancer cells that express high levels of EGFR and where surface EGFRs are not strongly downregulated because of saturation of the endocytosis and endosomal sorting machineries.

MATERIALS AND METHODS

Reagents

Human recombinant EGF was from BD Bioscience, TGFα was from Sigma (St Louis, MO, USA), HB-EGF and AR were from R&D Systems (Minneapolis, MN, USA). EGF–Rh was purchased from Molecular Probes (Eugene, OR, USA). Monoclonal antibodies to EEA.1 and rabbit polyclonal antibody to Shc were from BD Transduction Laboratories (San Diego, CA, USA); polyclonal antibody to Grb2 was from Santa Cruz Biotechnology Inc. (Santa Cruz, CA, USA); antibody 528 to EGFR (mAb528) was from ATCC (Manassas, VA, USA); monoclonal antibody to EGFR phosphotyrosine 1068 (pY1068), polyclonal antibodies to ERK1/2 and monoclonal antibody to phosphorylated ERK1/2 were from Cell Signaling Technology (Beverly, MA, USA). Polyclonal rabbit antibody to α-actinin was from Cell Signaling Technology. GFP antibody was from Abcam Inc. (Cambridge, MA, USA). PD158780 was from Calbiochem.

Cell culture

HeLa-Grb2–YFP cells (clone no.1) stably expressing shRNA-resistant Grb2–YFP and shRNA to Grb2 was previously described (Huang and Sorkin, 2005). HeLa-Grb2–YFP and parental HeLa cells were grown in Dulbecco's modified Eagle's medium (DMEM) containing 10% fetal bovine serum (FBS) and G418, all from Gibco, Life Bioscience. PAE cells were grown in F12 containing 10% FBS. For microscopy, the cells were grown on collagen-coated glass bottom plates (MatTek, Ashland, MA) and serum-starved for 16 hours. siRNA to ShcA was from Dharmacon, Inc. RNA interference experiments were performed as described previously (Goh et al., 2010).

Live-cell fluorescence microscopy

For time-lapse imaging MatTek dishes with HeLa-Grb2–YFP cells in 2 ml of binding medium (DMEM, 10 mM Hepes, 0.1% BSA) were

placed into the microscope stage adaptor, and z-stacks of confocal images were acquired using a spinning disk confocal imaging system based on a Zeiss Axio Observer Z1 inverted fluorescence microscope (with 63× Plan Apo PH NA 1.4 objective), equipped with a computer-controlled Spherical Aberration Correction unit, Yokogawa CSU-X1, Photometrics Evolve 16-bit EMCCD camera, environmental chamber and piezo stage controller and lasers (405, 445, 488, 515, 561 and 640 nm), all controlled by SlideBook 5.5 software (Intelligent Imaging Innovation, Denver, CO). Unless indicated otherwise, 22 serial two-dimensional confocal images at 500 nm intervals through 515 nm (YFP) and 561 nm (Rhodamine) channels were recorded in the environmental chamber, which ensured a constant temperature (37℃), humidity and 5% CO_2 atmosphere throughout the duration of imaging. EGF–Rh or unlabeled EGFR ligands were injected into the stage chamber in a large volume (0.2 ml), thus ensuring rapid distribution of ligands. The image integration time was 100 mseconds for both channels. Z-plane change time was ~3 mseconds. Total acquisition time for one two-channel 3D image was ~5.2 seconds. Intervals between image acquisition were 20–30 seconds during the first 10 minutes after ligand addition, and then images were acquired every 5 minutes or at the indicated times. All image acquisition settings were identical for experimental variants in each experiment. Time-lapse image sequences were corrected for photobleaching based on the 515 nm channel. No significant Rhodamine photobleaching was observed.

To estimate the amount of EGF–Rh and Grb2–YFP fluorescence in the plasma membrane and endosomes, 3D (22 planes) images of living HeLa-Grb2 cells were acquired at 37℃ at the indicated times after addition of EGF–Rh, as described above for time-lapse experiments. Background-subtracted 3D images were segmented to generate Mask 1, corresponding to the total YFP using the 3D object edge detection tool of SlideBook5.5, and Mask 2, corresponding to Rhodamine fluorescence using a minimal intensity threshold. Mask 1 was eroded (reduced) by 5 voxels from the entire surface of the mask using 3D erosion filtering to generate Mask 3, corresponding to intracellular voxels. Subtraction of Mask 3 from Mask 1 produced Mask 4 (surface voxels). Mask 4 and Mask 1 were merged with Mask 2 to select voxels that contained colocalized EGF–Rh and Grb2–YFP, and generate, respectively, 'Surface' (plasma membrane EGF–Rh and Grb2–YFP) and 'Inside' (endosomal EGF–Rh and Grb2–YFP) masks.

To quantify the stoichiometry of Grb2–YFP binding to EGFR, based on colocalization of YFP and EGF–Rh, 3D (22 planes), time-lapse images of living HeLa-Grb2–YFP cells were acquired at 37℃ at 5, 10, 15, 30 and 60 minutes after addition of EGF–Rh as described above. Calculations of the ratio of apparent fluorescence intensities of YFP and Rhodamine was performed based on voxel-to-voxel analysis of images of EGF–Rh and Grb2–YFP using the SlideBook5.5 statistics module. The background-subtracted 3D images were segmented to generate the 'total cell-associated' YFP mask (515 nm channel) and Rhodamine mask (561 nm channel) using minimal intensity thresholds. The 'colocalization' mask was generated by merging YFP and Rhodamine masks to select Grb2–YFP that was colocalized with EGF–Rh. The integrated voxel intensities of EGF–Rh and YFP in the 'colocalization' mask were calculated for individual cells or individual compartments (the plasma membrane and endosomes) by manually generating masks overlapping single cells in all z-planes. The total integrated intensity of the YFP mask was used to correct the YFP signal for photobleaching before the ratio of YFP to Rhodamine fluorescence intensity was calculated.

In parallel experiments, PAE cells transiently transfected with EGFR–YFP were incubated with 100 ng/ml EGF–Rh at 37℃ to saturate all receptors, and imaged under conditions identical to the imaging protocol used with HeLa-Grb2–YFP cells. Calculations of the apparent fluorescence intensities of YFP and Rhodamine corresponding to the equimolar ratio of EGFR–YFP and EGF–Rh were performed based on a voxel-to-voxel analysis of images of EGF–Rh and EGFR–YFP in PAE cells as described above for the Grb2–YFP:EGF–Rh ratio calculations. To quantify the molar ratio of Grb2–YFP to EGF–Rh, the values of the ratio of their apparent fluorescence intensities were divided by the value corresponding to the equimolar YFP:Rh ratio (~0.7) determined in PAE cells.

Quantification of Grb2–YFP subcellular distribution in fixed cells

As an additional approach to quantify relative amounts of Grb2–YFP associated with the plasma membrane and endosomes, the cells were incubated with 2 ng/ml EGF–Rh for the indicated times at 37℃ as described above, washed with ice-cold medium and incubated with mAb528 to occupy surface binding sites of EGFR at 4℃ for 1 hour. The cells were then fixed with freshly prepared 4% paraformaldehyde (Electron Microscopy Sciences, Washington, PA, USA) and further incubated with secondary anti-mouse antibody conjugated with Cy5. 3D images were acquired through 488 (Grb2–YFP), 561 (EGF–Rh) and 640 nm (mAb528) channels.

Three masks were generated by 3D segmentation of background-subtracted images: Mask488 (total cellular Grb2–YFP), Mask561 (total cellular EGF–Rh) and Mask640 (cell surface). Overlapping voxels of Mask488 and Mask640 correspond to MaskYFP-S (plasma membrane Grb2–YFP fluorescence). To generate MaskYFP-I corresponding to intracellular Grb2–YFP, MaskYFP-S was subtracted from MaskYFP. Merging the MaskYFP-I with Mask561 generated the 'End-Grb2–YFP' mask that corresponds to Grb2–YFP associated with endosomes containing EGF–Rh. Analysis of multiple images of cells not treated with EGF–Rh (time 0 of time-lapse experiments) showed that ~3% (±0.2%) of total cellular diffuse Grb2–YFP fluorescence overlaps with (or 'penetrates into') MaskYFP-S. Therefore, this non-specific fluorescence intensity (FI) was subtracted from the YFP FI of MaskYFP-S to obtain the specific FI of plasma-membrane-associated Grb2–YFP (pmYFP) for each image of cells treated with EGF–Rh using the equation:

$$I_{MaskYFP} - 0.03(FI_{MaskYFP} - FI_{MaskYFP-I}) = pmYFP. \quad (1)$$

The percentage of Grb2–YFP associated with the plasma membrane (PM Grb2–YFP) of the total Grb2–YFP colocalized with EGF–Rh was calculated using the equation:

$$\%PMGrb2-YFP = [pmYFP/(pmYFP + FI_{MaskYFP-I})]100. \quad (2)$$

Because EGF–Rh can be released from the cell surface during fixation and staining steps, the amount of surface EGF–Rh was not quantified.

Immunofluorescence microscopy

To determine the extent of colocalization of Grb2–YFP with EGFR and EEA.1, HeLa-Grb2–YFP cells grown on glass coverslips were treated with EGF or other unlabeled ligands at 37℃ for the indicated times, washed with ice-cold phosphate-buffered saline (PBS) and fixed with freshly prepared 4% paraformaldehyde. Cells were permeabilized with 0.1% Triton X-100 in PBS containing 0.1% BSA for 8 minutes, and incubated with mouse monoclonal EGFR (mAb528) or EEA.1 antibodies (1 hour at room temperature), followed by the secondary antibody conjugated with Cy3 (30 minutes). Cell nuclei were stained with 4′,6-diamidino-2-phenylindole (DAPI; 10 minutes) before coverslips were mounted on slides with Pro-Long Gold antifade reagent (Invitrogen).

Western blotting

To probe for active EGFR, Akt and ERK1/2, cells in six-well plates were serum-starved overnight, treated with EGF or other ligands at 37℃ for the indicated times, lysed in Triton X-100, glycerol, Hepes buffer in the presence of orthovanadate and *N*-ethyl-maleimide as described previously (Goh et al., 2010). The lysates were resolved by 7.5% SDS-PAGE followed by transfer to the nitrocellulose membrane. Western blotting was performed with appropriate primary and secondary antibodies conjugated to far-red fluorescent dyes (IRDye-680 and -800) followed by detection using the Odyssey LI-COR system. Quantifications were performed using LI-COR software.

^{125}I-EGF binding and internalization

Mouse receptor-grade EGF (Collaborative Research Inc., Bedford, MA, USA) was iodinated using a modified Chloramine T method as described previously (Sorkin and Duex, 2010). Binding and internalization of 2, 4

or 20 ng/ml ^{125}I-EGF at 37℃ was analyzed as described previously (Sorkin and Duex, 2010). For ligand competition experiments, cells were incubated with 0.5 ng/ml ^{125}I-EGF at 4℃ for 1 hour, washed in ice-cold DMEM and further incubated with unlabeled EGF or other EGFR ligands at the indicated concentrations at 4℃ for 1 hour. Quantifications of the ligand-binding sites per cell were performed as described previously (Sorkin and Duex, 2010).

Statistical analysis

The statistical significance (*P*-value) was calculated using unpaired two-tailed Student's *t*-tests (Prism 5 and Excel).

Acknowledgements

We thank Dr Colin Monks (Intelligent-Imaging Innovation) for help with developing the segmentation-based image analysis methodologies.

Competing interests

The authors declare no competing interests.

Author contributions

A.F. conceived, designed and conducted the experiments, analyzed the data and prepared the manuscript. A.S. conceived and designed the experiments, performed image analysis and prepared the manuscript.

Funding

This work was supported by the National Institutes of Health/National Cancer Institute [grant numbers CA112219 to A.F. and A.S. and CA089151 to A.S.]. Deposited in PMC for release after 12 months.

Supplementary material

Supplementary material available online at
http://jcs.biologists.org/lookup/suppl/doi:10.1242/jcs.137786/-/DC1

References

Adak, S., DeAndrade, D. and Pike, L. J. (2011). The tethering arm of the EGF receptor is required for negative cooperativity and signal transduction. *J. Biol. Chem.* **286**, 1545-1555.

Alvarado, D., Klein, D. E. and Lemmon, M. A. (2010). Structural basis for negative cooperativity in growth factor binding to an EGF receptor. *Cell* **142**, 568-579.

Baass, P. C., Di Guglielmo, G. M., Authier, F., Posner, B. I. and Bergeron, J. J. (1995). Compartmentalized signal transduction by receptor tyrosine kinases. *Trends Cell Biol.* **5**, 465-470.

Batzer, A. G., Rotin, D., Ureña, J. M., Skolnik, E. Y. and Schlessinger, J. (1994). Hierarchy of binding sites for Grb2 and Shc on the epidermal growth factor receptor. *Mol. Cell. Biol.* **14**, 5192-5201.

Brankatschk, B., Wichert, S. P., Johnson, S. D., Schaad, O., Rossner, M. J. and Gruenberg, J. (2012). Regulation of the EGF transcriptional response by endocytic sorting. *Sci. Signal.* **5**, ra21.

Carpenter, G. and Cohen, S. (1979). Epidermal growth factor. *Annu. Rev. Biochem.* **48**, 193-216.

Chen, Z., Gibson, T. B., Robinson, F., Silvestro, L., Pearson, G., Xu, B., Wright, A., Vanderbilt, C. and Cobb, M. H. (2001). MAP kinases. *Chem. Rev.* **101**, 2449-2476.

Chook, Y. M., Gish, G. D., Kay, C. M., Pai, E. F. and Pawson, T. (1996). The Grb2-mSos1 complex binds phosphopeptides with higher affinity than Grb2. *J. Biol. Chem.* **271**, 30472-30478.

Di Fiore, P. P. and De Camilli, P. (2001). Endocytosis and signaling. an inseparable partnership. *Cell* **106**, 1-4.

Di Guglielmo, G. M., Baass, P. C., Ou, W.-J., Posner, B. I. and Bergeron, J. J. M. (1994). Compartmentalization of SHC, GRB2 and mSOS, and hyperphosphorylation of Raf-1 by EGF but not insulin in liver parenchyma. *EMBO J.* **13**, 4269-4277.

Diwan, B. A., Ramakrishna, G., Anderson, L. M. and Ramljak, D. (2000). Overexpression of Grb2 in inflammatory lesions and preneoplastic foci and tumors induced by N-nitrosodimethylamine in Helicobacter hepaticus-infected and -noninfected A/J mice. *Toxicol. Pathol.* **28**, 548-554.

Ebner, R. and Derynck, R. (1991). Epidermal growth factor and transforming growth factor-alpha: differential intracellular routing and processing of ligand-receptor complexes. *Cell Regul.* **2**, 599-612.

Eden, E. R., Huang, F., Sorkin, A. and Futter, C. E. (2012). The role of EGF receptor ubiquitination in regulating its intracellular traffic. *Traffic* **13**, 329-337.

French, A. R., Sudlow, G. P., Wiley, H. S. and Lauffenburger, D. A. (1994). Postendocytic trafficking of epidermal growth factor-receptor complexes is mediated through saturable and specific endosomal interactions. *J. Biol. Chem.* **269**, 15749-15755.

French, A. R., Tadaki, D. K., Niyogi, S. K. and Lauffenburger, D. A. (1995). Intracellular trafficking of epidermal growth factor family ligands is directly influenced by the pH sensitivity of the receptor/ligand interaction. *J. Biol. Chem.* **270**, 4334-4340.

Galperin, E., Verkhusha, V. V. and Sorkin, A. (2004). Three-chromophore FRET microscopy to analyze multiprotein interactions in living cells. *Nat. Methods* **1**, 209-217.

Gillham, H., Golding, M. C., Pepperkok, R. and Gullick, W. J. (1999). Intracellular movement of green fluorescent protein-tagged phosphatidylinositol 3-kinase in response to growth factor receptor signaling. *J. Cell Biol.* **146**, 869-880.

Goh, L. K., Huang, F., Kim, W., Gygi, S. and Sorkin, A. (2010). Multiple mechanisms collectively regulate clathrin-mediated endocytosis of the epidermal growth factor receptor. *J. Cell Biol.* **189**, 871-883.

Haugh, J. M. and Meyer, T. (2002). Active EGF receptors have limited access to PtdIns(4,5)P(2) in endosomes: implications for phospholipase C and PI 3-kinase signaling. *J. Cell Sci.* **115**, 303-310.

Huang, F. and Sorkin, A. (2005). Growth factor receptor binding protein 2-mediated recruitment of the RING domain of Cbl to the epidermal growth factor receptor is essential and sufficient to support receptor endocytosis. *Mol. Biol. Cell* **16**, 1268-1281.

Imai, Y., Leung, C. K., Friesen, H. G. and Shiu, R. P. (1982). Epidermal growth factor receptors and effect of epidermal growth factor on growth of human breast cancer cells in long-term tissue culture. *Cancer Res.* **42**, 4394-4398.

Jiang, X. and Sorkin, A. (2002). Coordinated traffic of Grb2 and Ras during epidermal growth factor receptor endocytosis visualized in living cells. *Mol. Biol. Cell* **13**, 1522-1535.

Jiang, X., Huang, F., Marusyk, A. and Sorkin, A. (2003). Grb2 regulates internalization of EGF receptors through clathrin-coated pits. *Mol. Biol. Cell* **14**, 858-870.

Johannessen, L. E., Haugen, K. E., Østvold, A. C., Stang, E. and Madshus, I. H. (2001). Heterodimerization of the epidermal-growth-factor (EGF) receptor and ErbB2 and the affinity of EGF binding are regulated by different mechanisms. *Biochem. J.* **356**, 87-96.

Kranenburg, O., Verlaan, I. and Moolenaar, W. H. (1999). Dynamin is required for the activation of mitogen-activated protein (MAP) kinase by MAP kinase kinase. *J. Biol. Chem.* **274**, 35301-35304.

Lemmon, M. A. and Schlessinger, J. (2010). Cell signaling by receptor tyrosine kinases. *Cell* **141**, 1117-1134.

Lemmon, M. A., Ladbury, J. E., Mandiyan, V., Zhou, M. and Schlessinger, J. (1994). Independent binding of peptide ligands to the SH2 and SH3 domains of Grb2. *J. Biol. Chem.* **269**, 31653-31658.

Low-Nam, S. T., Lidke, K. A., Cutler, P. J., Roovers, R. C., van Bergen en Henegouwen, P. M., Wilson, B. S. and Lidke, D. S. (2011). ErbB1 dimerization is promoted by domain co-confinement and stabilized by ligand binding. *Nat. Struct. Mol. Biol.* **18**, 1244-1249.

Lowenstein, E. J., Daly, R. J., Batzer, A. G., Li, W., Margolis, B., Lammers, R., Ullrich, A., Skolnik, E. Y., Bar-Sagi, D. and Schlessinger, J. (1992). The SH2 and SH3 domain-containing protein GRB2 links receptor tyrosine kinases to ras signaling. *Cell* **70**, 431-442.

Matsuda, M., Paterson, H. F., Rodriguez, R., Fensome, A. C., Ellis, M. V., Swann, K. and Katan, M. (2001). Real time fluorescence imaging of PLC gamma translocation and its interaction with the epidermal growth factor receptor. *J. Cell Biol.* **153**, 599-612.

Miaczynska, M., Pelkmans, L. and Zerial, M. (2004). Not just a sink: endosomes in control of signal transduction. *Curr. Opin. Cell Biol.* **16**, 400-406.

Morimatsu, M., Takagi, H., Ota, K. G., Iwamoto, R., Yanagida, T. and Sako, Y. (2007). Multiple-state reactions between the epidermal growth factor receptor and Grb2 as observed by using single-molecule analysis. *Proc. Natl. Acad. Sci. USA* **104**, 18013-18018.

Nag, A., Monine, M. I., Faeder, J. R. and Goldstein, B. (2009). Aggregation of membrane proteins by cytosolic cross-linkers: theory and simulation of the LAT-Grb2-SOS1 system. *Biophys. J.* **96**, 2604-2623.

Nexø, E. and Hansen, H. F. (1985). Binding of epidermal growth factor from man, rat and mouse to the human epidermal growth factor receptor. *Biochim. Biophys. Acta* **843**, 101-106.

Okabayashi, Y., Kido, Y., Okutani, T., Sugimoto, Y., Sakaguchi, K. and Kasuga, M. (1994). Tyrosines 1148 and 1173 of activated human epidermal growth factor receptors are binding sites of Shc in intact cells. *J. Biol. Chem.* **269**, 18674-18678.

Oksvold, M. P., Skarpen, E., Wierød, L., Paulsen, R. E. and Huitfeldt, H. S. (2001). Re-localization of activated EGF receptor and its signal transducers to multivesicular compartments downstream of early endosomes in response to EGF. *Eur. J. Cell Biol.* **80**, 285-294.

Okutani, T., Okabayashi, Y., Kido, Y., Sugimoto, Y., Sakaguchi, K., Matuoka, K., Takenawa, T. and Kasuga, M. (1994). Grb2/Ash binds directly to tyrosines 1068 and 1086 and indirectly to tyrosine 1148 of activated human epidermal growth factor receptors in intact cells. *J. Biol. Chem.* **269**, 31310-31314.

Roepstorff, K., Grandal, M. V., Henriksen, L., Knudsen, S. L., Lerdrup, M., Grøvdal, L., Willumsen, B. M. and van Deurs, B. (2009). Differential effects of EGFR ligands on endocytic sorting of the receptor. *Traffic* **10**, 1115-1127.

Sato, K., Kimoto, M., Kakumoto, M., Horiuchi, D., Iwasaki, T., Tokmakov, A. A. and Fukami, Y. (2000). Adaptor protein Shc undergoes translocation and mediates up-regulation of the tyrosine kinase c-Src in EGF-stimulated A431 cells. *Genes Cells* **5**, 749-764.

Scaltriti, M. and Baselga, J. (2006). The epidermal growth factor receptor pathway: a model for targeted therapy. *Clin. cancer res.* **12**, 5268-5272.

Schulze, W. X., Deng, L. and Mann, M. (2005). Phosphotyrosine interactome of the ErbB-receptor kinase family. *Mol. Syst. Biol.* **1**, 0008.

Scita, G. and Di Fiore, P. P. (2010). The endocytic matrix. *Nature* **463**, 464-473.

Sibilia, M., Kroismayr, R., Lichtenberger, B. M., Natarajan, A., Hecking, M. and Holcmann, M. (2007). The epidermal growth factor receptor: from development to tumorigenesis. *Differentiation* **75**, 770-787.
Sorkin, A. and Duex, J. E. (2010). Quantitative analysis of endocytosis and turnover of epidermal growth factor (EGF) and EGF receptor. *Curr. Protoc. Cell Biol.* **46**, 15.14.1-15.14.20.
Sorkin, A. and Goh, L. K. (2009). Endocytosis and intracellular trafficking of ErbBs. *Exp. Cell Res.* **315**, 683-696.
Sorkin, A. and von Zastrow, M. (2002). Signal transduction and endocytosis: close encounters of many kinds. *Nat. Rev. Mol. Cell Biol.* **3**, 600-614.
Sorkin, A. and von Zastrow, M. (2009). Endocytosis and signalling: intertwining molecular networks. *Nat. Rev. Mol. Cell Biol.* **10**, 609-622.
Sorkin, A., Waters, C. M., Overholser, K. A. and Carpenter, G. (1991). Multiple autophosphorylation site mutations of the epidermal growth factor receptor. Analysis of kinase activity and endocytosis. *J. Biol. Chem.* **266**, 8355-8362.
Sorkin, A., McClure, M., Huang, F. and Carter, R. (2000). Interaction of EGF receptor and grb2 in living cells visualized by fluorescence resonance energy transfer (FRET) microscopy. *Curr. Biol.* **10**, 1395-1398.
Sousa, L. P., Lax, I., Shen, H., Ferguson, S. M., De Camilli, P. and Schlessinger, J. (2012). Suppression of EGFR endocytosis by dynamin depletion reveals that EGFR signaling occurs primarily at the plasma membrane. *Proc. Natl. Acad. Sci. USA* **109**, 4419-4424.
Verbeek, B. S., Adriaansen-Slot, S. S., Rijksen, G. and Vroom, T. M. (1997). Grb2 overexpression in nuclei and cytoplasm of human breast cells: a histochemical and biochemical study of normal and neoplastic mammary tissue specimens. *J. Pathol.* **183**, 195-203.
Vieira, A. V., Lamaze, C. and Schmid, S. L. (1996). Control of EGF receptor signaling by clathrin-mediated endocytosis. *Science* **274**, 2086-2089.
Vlodavsky, I., Brown, K. D. and Gospodarowicz, D. (1978). A comparison of the binding of epidermal growth factor to cultured granulosa and luteal cells. *J. Biol. Chem.* **253**, 3744-3750.
Waterman, H., Katz, M., Rubin, C., Shtiegman, K., Lavi, S., Elson, A., Jovin, T. and Yarden, Y. (2002). A mutant EGF-receptor defective in ubiquitylation and endocytosis unveils a role for Grb2 in negative signaling. *EMBO J.* **21**, 303-313.
Wells, A., Welsh, J. B., Lazar, C. S., Wiley, H. S., Gill, G. N. and Rosenfeld, M. G. (1990). Ligand-induced transformation by a noninternalizing epidermal growth factor receptor. *Science* **247**, 962-964.
Wiley, H. S. and Cunningham, D. D. (1982). The endocytotic rate constant. A cellular parameter for quantitating receptor-mediated endocytosis. *J. Biol. Chem.* **257**, 4222-4229.
Wouters, F. S. and Bastiaens, P. I. (1999). Fluorescence lifetime imaging of receptor tyrosine kinase activity in cells. *Curr. Biol.* **9**, 1127-1130.

Journal of Cell Science

Fortian and Sorkin J. Cell Science

SUPPLEMENTAL MATERIALS

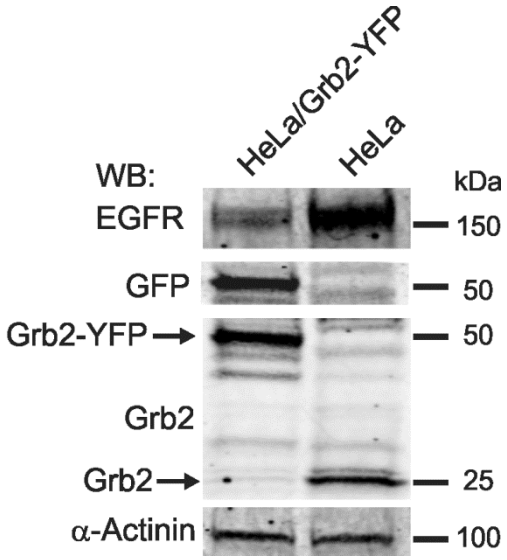

Figure S1. Western blot analysis of Grb2-YFP and Grb2 expression in parental HeLa and HeLa/Grb2-YFP cells.

Equal amounts of lysates of HeLa and HeLa/Grb2-YFP cells were resolved by SDS-PAGE, and probed by western blotting with antibodies to Grb2, GFP, EGFR and α-actinin (loading control). The amount of Grb2 immunoreactivity was 2.13-fold higher in HeLa/Grb2-YFP than in parental HeLa cells.

Figure S2. Time-lapse imaging of Grb2-YFP in cells stimulated with 20 ng/ml EGF-Rh (0-60 min) (Next page)

3D time-lapse imaging of HeLa/Grb2-YFP cells was performed during the first hour after addition of 20 ng/ml EGF-Rh to cells at 37°C with 5-min intervals between frames as described in "Methods". Selected time lapse x-y and x-z images are presented. Arrows point on examples of co-localization of EGF-Rh and Grb2-YFP in endosomes. Scale bar, 10 μm.

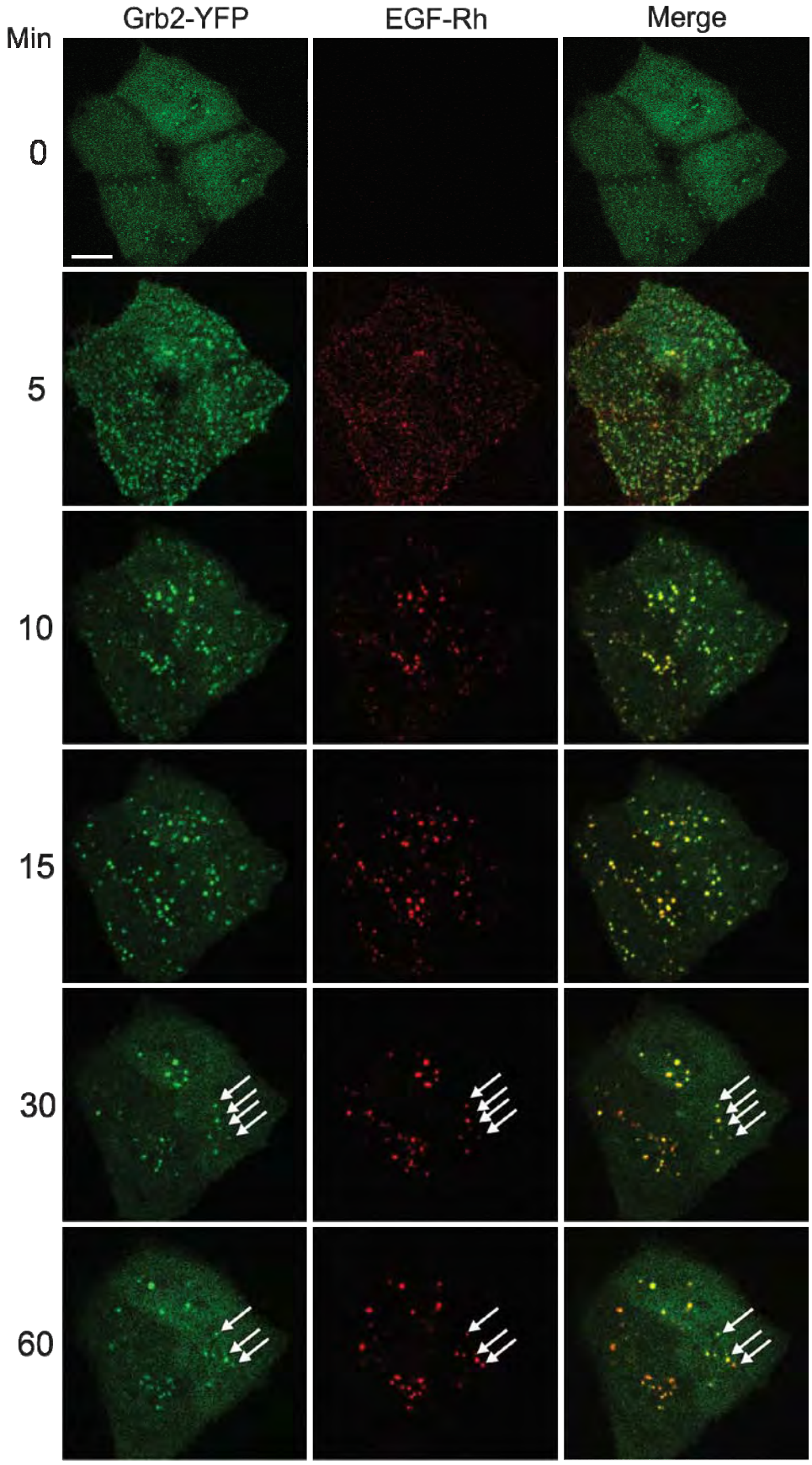
Min
Grb2-YFP
EGF-Rh
Merge
0
5
10
15
30
60

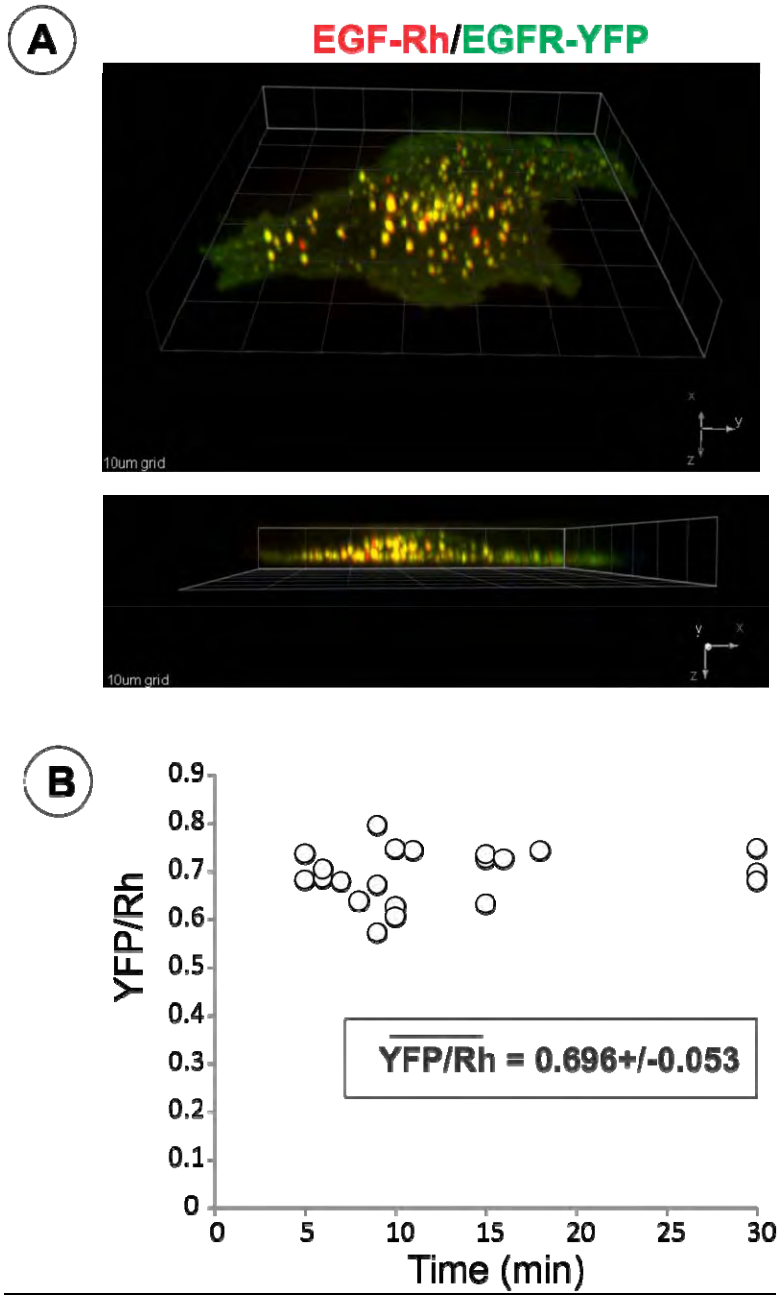

Figure S3. Apparent fluorescence intensity ratio of YFP and rhodamine in equimolar EGFR-YFP/EGF-Rh complexes.

(**A**) PAE cells transiently expressing EGFR-YFP were incubated with 100 ng/ml of EGF-Rh for 5-30 min at 37^{o}C. Live-cell 3-D imaging was performed through 515 and 561 channels as described in Figs. 1 and 2. An example of a 3-D image (two different views) of a cell incubated with EGF-Rh for 30 min is presented. Grid, 10 μm.

(**B**) Calculations of the ratio of YFP to rhodamine fluorescence (YFP/Rh) in 3-D images of cells exemplified in (***A***) were performed as described in "Methods". Each data point represents an individual cell.

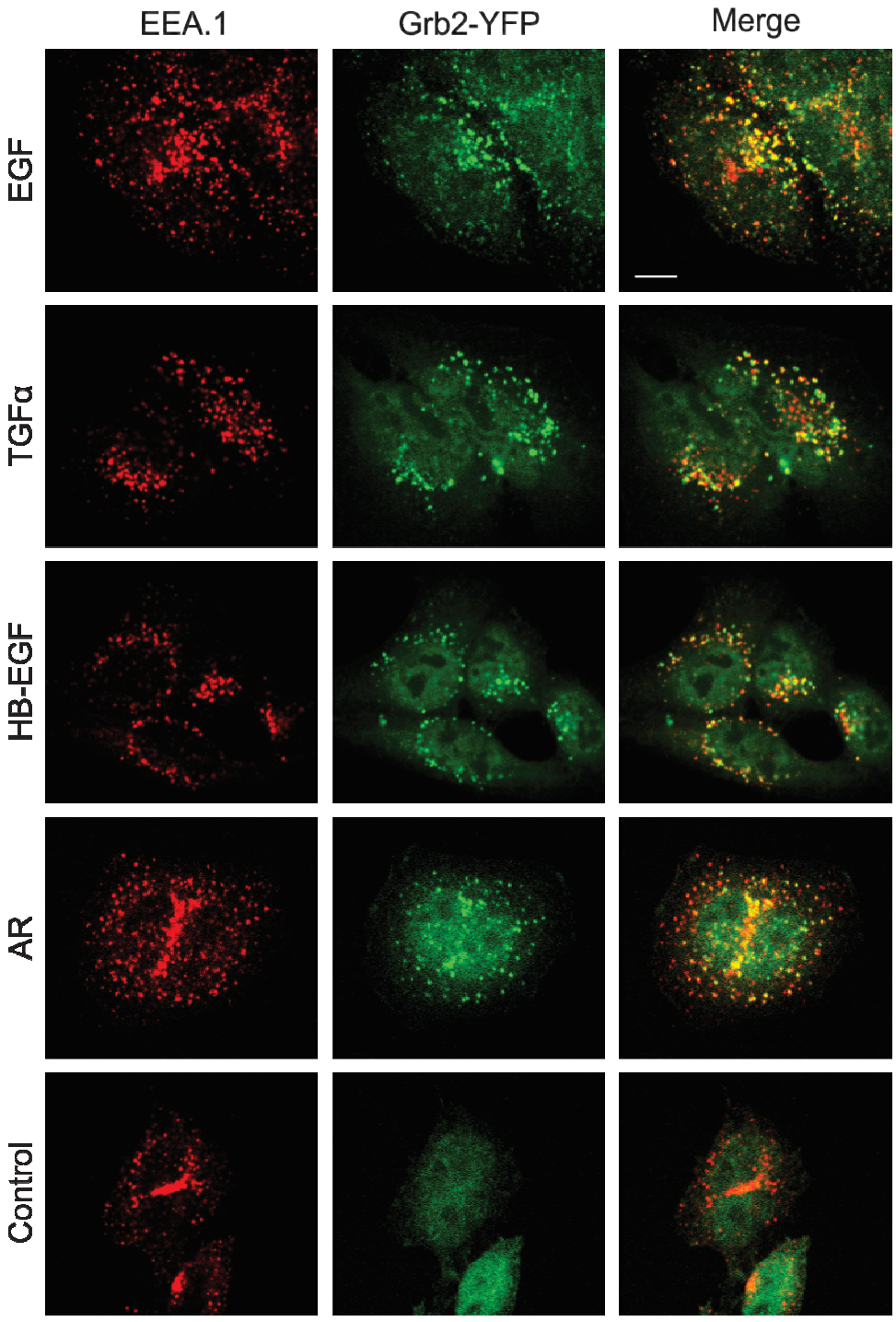

Figure S4. Colocalization of Grb2-YFP with EEA.1 in HeLa/Grb2-YFP cells treated with various unlabeled EGFR ligands.

Cells grown on glass coverslips were left untreated (***Control***) or treated with EGF (2 ng/ml), TGFα (2 ng/ml), HB-EGF (2 ng/ml) or AR (400 ng/ml) at 37°C for 30 min, fixed and stained with mouse monoclonal antibody to EEA.1 followed by the secondary antibody conjugated with Cy3. Scale bar, 10 μm.

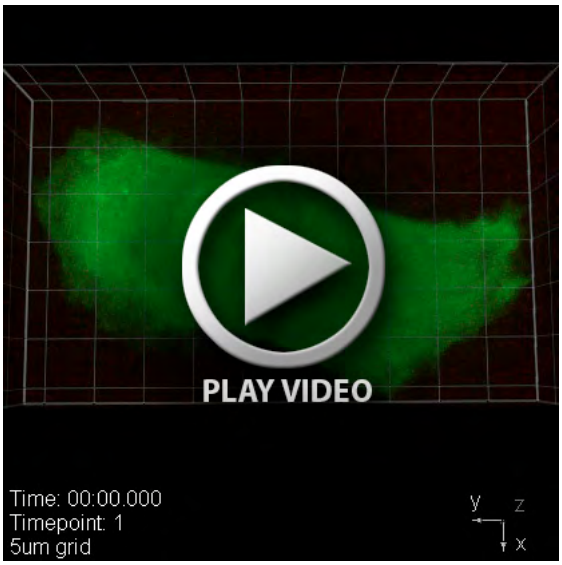

Movie 1. 3D time-lapse movie sequence of HeLa/Grb2-YFP cells treated with EGF-Rh. x-y-z view of the 3D time-lapse image sequence presented in Figure 1. The cells were incubated with 2 ng/ml EGF-Rh for 0-10 min. Merged Rhodamine (red) and YFP (green) images are shown.

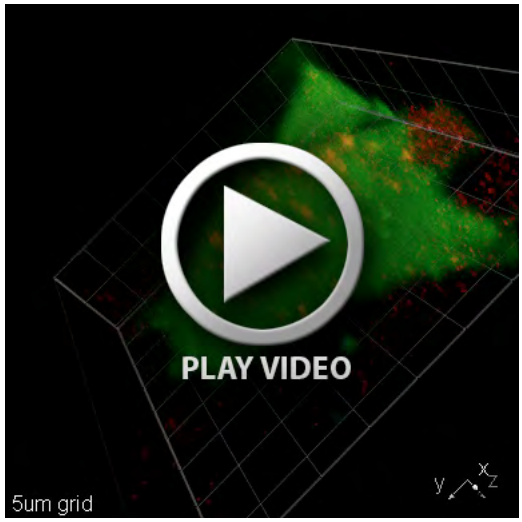

Movie 2. HeLa/Grb2-YFP cells incubated with EGF-Rh for 5 min. 160 degrees rotational 3D-view of a cell treated with 2 ng/ml EGF-Rh for 5 min from the time-lapse imaging sequence presented in Figure 2. Merged Rhodamine (red) and YFP (green) image is shown.

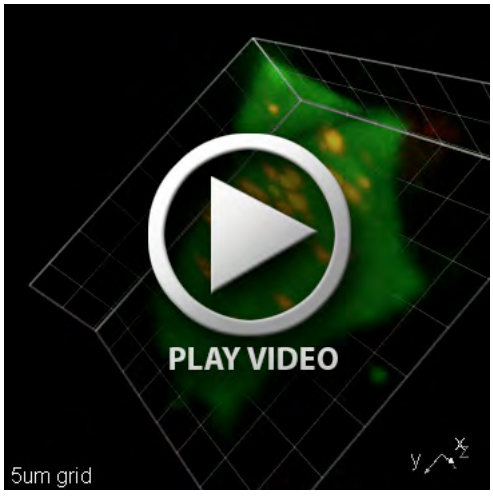

Movie 3. HeLa/Grb2-YFP cells incubated with EGF-Rh for 30 min. 160 degrees rotational 3D-view of a cell treated with 2 ng/ml EGF-Rh for 30 min from the time-lapse imaging sequence presented in Figure 2. Merged Rhodamine (red) and YFP (green) image is shown.